CHAPTER 1

INTRODUCTION

1.1 General Background

The main problems in failure of a component are initiation and propagation of cracks. Sliding contact is one of the causes that may lead to those problems. The initiation, later, will lead to fretting fatigue and can damage the component [1]. The stresses, including normal and shear stress can be measured using numerical procedure and asymptotic forms, and it is recommended to use both methods to achieve a greater understanding of the contact.

1.2 Problem Statement

There are certain areas of the contact that experience high stress intensity during sliding between two bodies. These areas need to be identified to prevent cracking from occurring to the contact surface.

1.3 Objectives

The main objective of the project is to analyze the stress at the contacting surface, at the edge of the contact and in the subsurface when a square punch is sliding on top of an elastically similar half-plane. Apart from that, the most critical areas that experience greatest stress during sliding need to be identified.

1.4 Scope of Study

This project is conducted to study the sliding contact problems between two elastically similar bodies using ANSYS. For this project, ANSYS can be used to simulate the stress distribution of the contacting bodies when the punch is sliding.

The results obtained from ANSYS, was compared to numerical method to determine whether the results are correct or not. The simulation was repeated until it gives the correct solutions, compared to previous studies.

There are many studies about different angle of the punch sliding on top of an elastically similar half-plane, for instance, 60˚ and 120˚ punch, but in this project, it will only be covering 90˚ punch.

CHAPTER 2

LITERATURE REVIEW / THEORY

2.1 Sliding Contact's Modeling

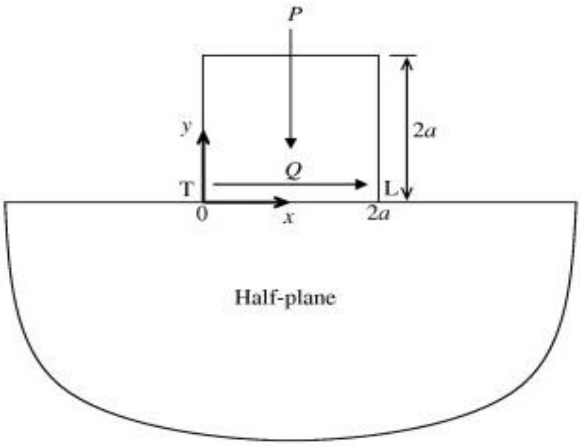

Figure 2.1: Elastic square punch sliding on an elastically similar half-plane

Figure 2.1 above shows the model of the sliding contact problem, which consists of one 90˚ square punch and a half plane [2]. Both punch and the half plane are made from the same material and having the same material properties.

From the figure above, *P* represents the normal force applied on the punch that is pressed onto the half plane. Meanwhile, *Q* is the shearing force, acting horizontally to the punch, with some value of coefficient of friction, *f* along the contact surface between the two bodies [3]. To cause the square block to slide, *Q* needs to be equal or greater than the multiplication of *P* and *f*.

Shearing force ≥ coefficient of friction * normal force

2.2 Stress Analysis Using Finite Element Analysis (FEA)

Numerical methods develop the governing equations, normally used to solve partial differential equations. It divides complicated problem into a smaller ones, which can be solved in relation to each other. When applied to real-life problem situations it is often difficult to obtain an exact solution to those equations in view of complex geometry and boundary conditions. The finite element method can be viewed simply as a method of finding approximate solution for partial differential equations or as a tool to transform partial equations into algebraic equations, which are then easily solved [4].

To achieve a better understanding of the stress analysis, it is recommended to combine both finite elements together with asymptotic forms [3]. But in this project, only finite element will be implemented using finite element computer software called ANSYS.

2.3 Asymptotic Analysis

To analyze the sliding contacts of two elastically similar bodies using asymptotic forms, the characteristic equation given below is used [2][3].

$$\nabla(\varphi, f, \alpha, \beta; \lambda) = (1+\alpha)cos\lambda\pi(sin^2\lambda\varphi - \lambda^2 sin^2\varphi) + \frac{1}{2}(1-\alpha)\sin\lambda\pi\,(sin2\lambda\varphi - \lambda sin2\varphi) + f sin\lambda\pi\,[(1-\alpha)\lambda(1+\lambda)sin^2\varphi - 2\beta(sin^2\varphi - \lambda^2 sin^2\varphi)] = 0 \qquad (1)$$

where α and β are the Dundurs parameters, φ is the internal angle, f is the coefficient of friction on the contact surface and λ is the slipping eigenvalues.

Due to the fact that both of the punch and half-plane is assumed to be elastically similar, the Dundurs parameters, will be zero [2]. Since our analysis is only covering a square punch, the value of internal angle must be 90°. Therefore, the equation above becomes

$$\left(sin^2\left[\frac{\lambda\pi}{2}\right] - \lambda^2\right)\cos[\lambda\pi] + \frac{1}{2}sin^2[\lambda\pi] + f\lambda(1+\lambda)\sin[\lambda\pi] = 0 \qquad (2)$$

The equation above is only applicable for a square punch sliding on an elastically similar half-plane. The only unknowns are coefficient of friction, which can be manipulated in this analysis, and also the slipping eigenvalues. This equation leads to the graph below [2][3].

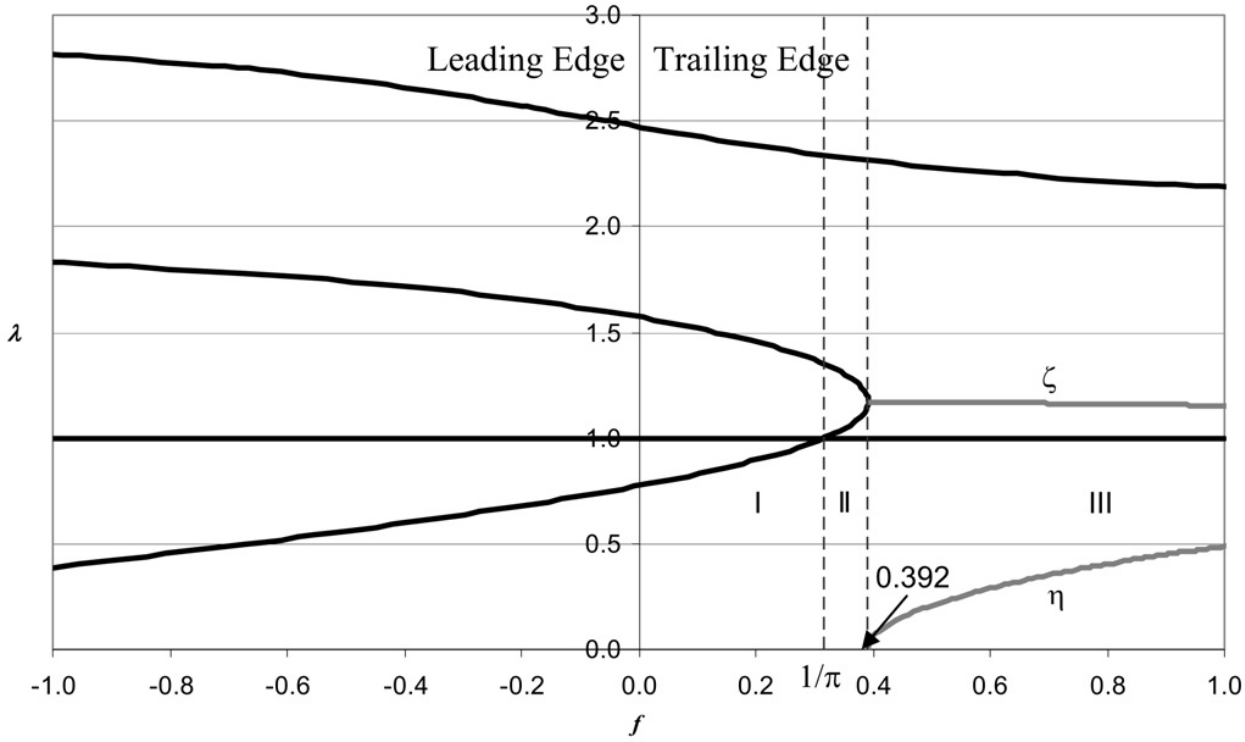

Figure 2.2: The slipping eigenvalues , λ as the function of the coefficient of friction, f [2][3].

In Figure 2.2, the graph is divided into two parts, which are leading edge and trailing edge. At the leading edge side, it is easier to understand since the behavior is power order singular [3]. Meanwhile at the trailing side, it is a little bit more complicated to analyze. There are three regions at the trailing side that shows different characteristics than the other region.

When the coefficient of friction is less than $\frac{1}{\pi}$, approximately 0.318 (Region 1), the behavior is still power order singular, which means the real root is always between 0 and 1. In this region, the contact pressure can be written in the form of

$$p(r) = -\sigma_{\theta\theta}(r,0) = K_s r^{\lambda_s - 1} \tag{3}$$

where K_s is the generalized stress intensity factor and r is the coordinate measured from the contact edge.

In the Region 2, where the coefficient of friction is between 0.318 and 0.392, it is clear that there are two real roots in the interval $1 < \lambda < 2$. So the contact pressure is

$$p(r) = -\sigma_{\theta\theta}(r,0) = K_{b1} r^{\lambda b1 - 1} + K_{b2} r^{\lambda b2 - 1} \tag{4}$$

where K_{b1} and K_{b2} are the stress intensity factors [3].

In the Region 3, where the coefficient of friction exceeds 0.392, the real root is within the interval $2 < \lambda < 3$. Not just that, there is a complex root with a smaller real part within $1 < \lambda < 2$. The contact pressure can be written in the form of

$$p(r) = -\sigma_{\theta\theta}(r,0) = K_c r^{\zeta - 1} sin\left[\eta \ln\left(\frac{r}{r_0}\right)\right], 1 < \zeta < 2, 0 < \eta < 1 \tag{5}$$

where K_c is the stress intensity, ζ and η are the real and imaginary parts of the eigenvalue.

CHAPTER 3

METHODOLOGY

3.1 Project Activities and Key Milestone

Several targets were set for the FYP I and FYP II. Table 3.1 and Table 3.2 show the project activities and key milestones for FYP I and FYP II respectively.

Table 3.1: Project Activities and Key Milestones for FYP I

No.	Detail/ Week	1	2	3	4	5	6	7		8	9	10	11	12	13	14
1	Selection of Project Topic	■														
2	Literatures Review		■	■	■	■										
3	Submission of Extended Proposal						●									
4	Recap about ANSYS							■		■						
5	Proposal Defense Presentation										●					
6	Simulation using ANSYS											■	■	■	■	
7	Generating proper models											■	■	■	■	
8	Submission of Interim Draft Report														●	
9	Submission of Interim Report															●

MID SEM BREAK

Legends:

■ Project Activity

● Key Milestone

Table 3.2: Project Activities and Key Milestones for FYP II

	Detail/ Week	1	2	3	4	5	6	7		8	9	10	11	12	13	14	15
1	Simulation using ANSYS	■	■	■	■	■	■	■		■	■	■	■				
2	Analyze stress at subsurface												■	■	■		
3	Submission of Progress Report									■○							
									MID SEM BREAK								
4	Pre-SEDEX												■○				
5	Submission of Draft Report													■○			
6	Submission of Dissertation (soft bound)														■○		
7	Submission of Technical Paper														■○		
8	Oral Presentation															■○	
9	Submission of Project Dissertation (Hard Bound)																■○

Legends:

■ Project Activity

■○ Key Milestone

3.2 Procedure Flow Chart

Figure 3.1 below shows the procedure flow chart of the project.

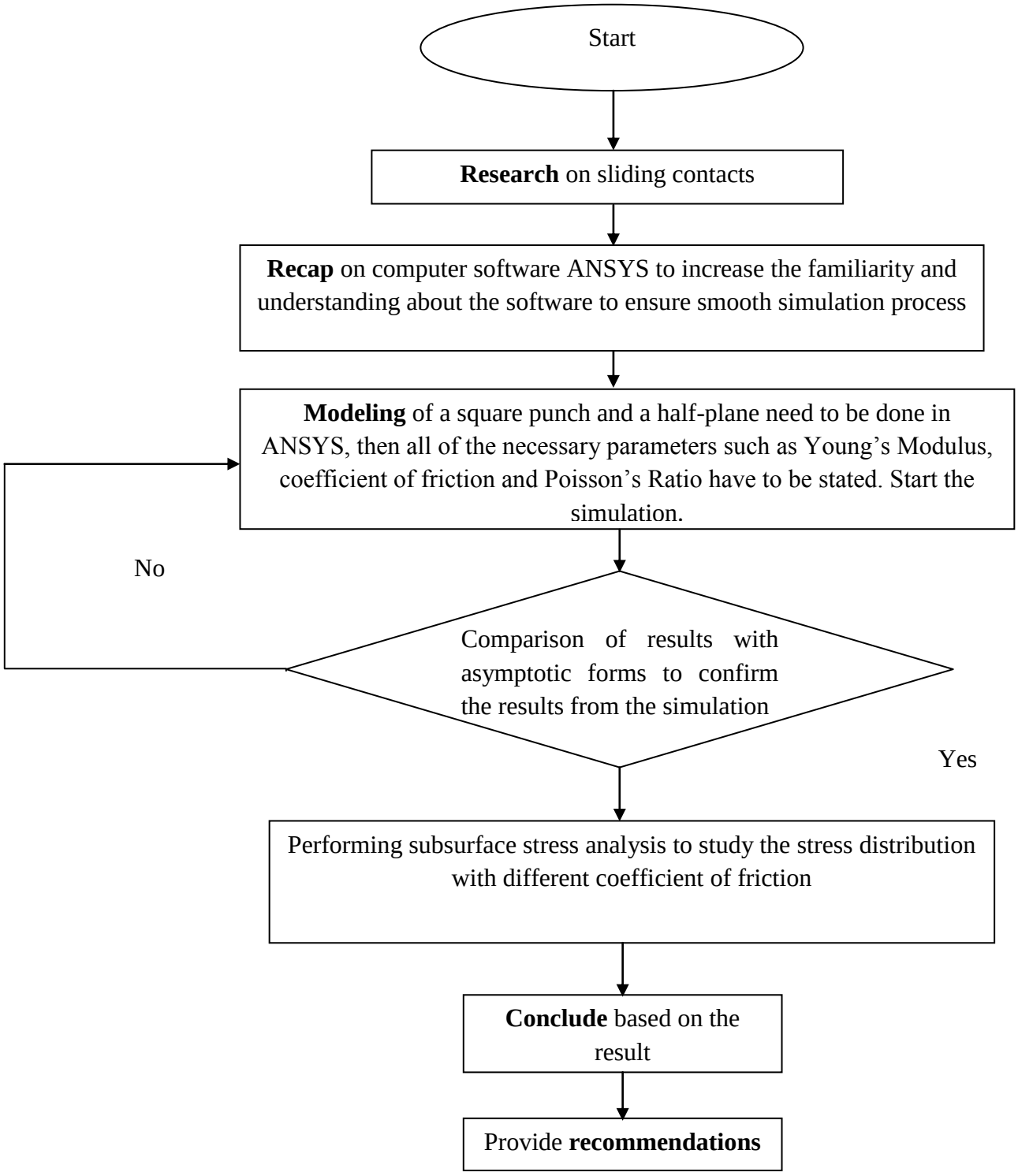

Figure 3.1: Procedure Flow Chart

3.3 Contact Analysis

There are 3 major steps in performing simulation using ANSYS, which are pre-processor, processor and post-processor. Basically, pre-processor is the stage where the user has to define the problem. Some parameters need to be provided in this stage before entering the processor phase. For instance, Poisson's ratio and the material's Young's Modulus. Plus, this is the stage where the contact pair is created.

In processor, loads are defined to the model. Some boundary conditions are also applied in this phase. Users may start the simulation in this phase.

Post-processor is just a phase where users may view the results. There are many kinds of results that can be viewed such as distribution of contact pressure and frictional stress along the contact interface. Contour plot is a very common choice for users to view the stress distribution on the model.

Below are the steps required to achieve the results needed from ANSYS in this project.

1. Create the model

Pre-processor – Modeling – Create – Area – Rectangle – By Dimension

Table 3.3: Dimension of Square Punch and Half-plane

ELEMENT	DIMENSION
Square punch	(X1 = 9, X2 = 11) (Y1 = 10, Y2 = 12)
Half-plane	(X1 = 0, X2 = 20) (Y1 = 0, Y2 = 10)

Table 3.3 shows the coordinates that need to be defined to create both punch and half-plane.

2. Define Material Properties

Pre-processor – Material Properties – Material Models – Structural – Linear – Elastic – Isotropic

Table 3.4: Material Properties of Contact Model

Young's Modulus (EX)	115 GPa
Poisson's Ratio (PRXY)	0.33

Table 3.4 shows the value of Young's Modulus and Poisson's Ratio used in this project. These are the properties of a typical titanium alloy.

3. Define Element Type

Pre-processor – Element type – Add/Edit/Delete

For this project, it is recommended to use Structural Mass Solid, PLANE42 element. This is because the element has two degree of freedom at the nodes and the element in two dimensional, which is suitable for this analysis.

4. Set Mesh Size

Pre-processor – Meshing – Size Controls – Manual Size – Areas - All Areas

For a start, it is enough to select an edge length of 1. It may not provide the best results, but it is faster to simulate the result. But if the user wants to obtain the results as accurate as possible, then he/she should key in a smaller number, 0.1 for instance.

5. Generate Mesh

Pre-processor – Meshing – Mesh – Areas – Free – Picked All

After this step, the users will have their preferred mesh size on the elements that they selected.

6. Create Contact Pair

Pre-processor – Modeling – Create Contact Pair

This step requires the user to use Contact Wizard. The user will have to define the contact and the target, which is punch and half-plane, respectively. Usually, the harder material will be best considered as the contact, but in this case, both of the elements are from the same material, thus they possess the same properties.

7. Define Boundary Limit

Solution – Define Loads – Apply – Structural – Displacement – On Lines

Select the bottom end of the half-plane. This is basically to constrain all degrees of freedom there, which means it will not move or no displacement whatsoever.

8. Apply Loads

Solution – Define Loads – Apply – Structural – Pressure – On Lines

Apply pressure of 50 N/m^2 on the top of the square punch, vertically downwards. This represents the normal force acting on the punch. After that, for f = 0.1, apply shearing force of 10 N on the top left side of the punch to represent the shearing force. To avoid the punch from tilting, the moment must be neutralized by applying 10 N upward on the top right side and 10 N downward on the top left side of the punch.

9. Solve

Solution – Solve – Current LS

CHAPTER 4

RESULTS

4.1 Surface Stress Analysis

For surface stress analysis, there are four main parameters related to this project. After performing the steps in methodology, these are the parameters that need to be obtained.

- SY – stress in Y-direction
- SXY – stress in XY-direction
- Contact Pressure (contpress) along the contact interface
- Contact Frictional Stress (contfri) along the contact interface

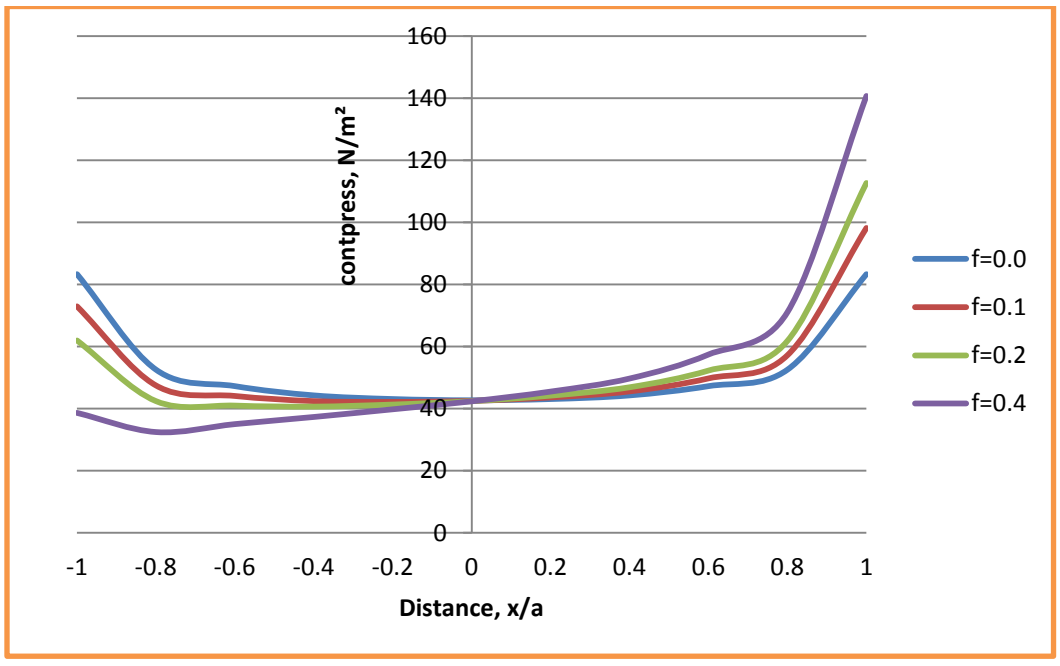

Figure 4.1: Distribution of contact pressure along the contact interface (*f*=0.0 to *f*=0.4)

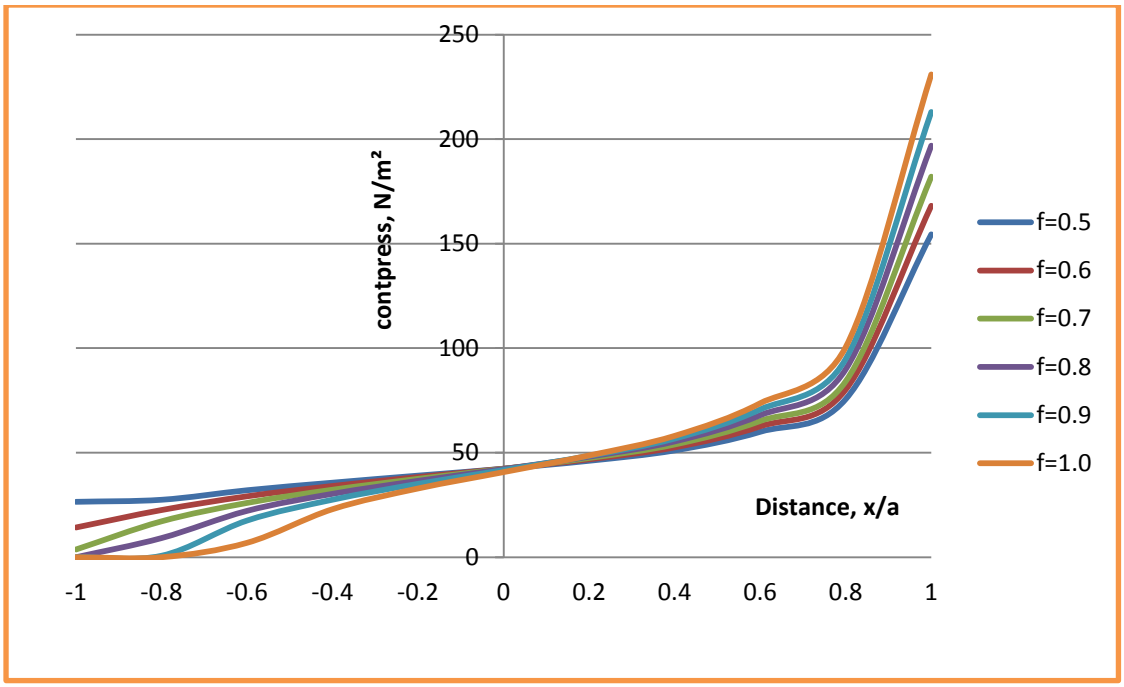

Figure 4.2: Distribution of contact pressure along the contact interface (*f*=0.5 to *f*=1.0)

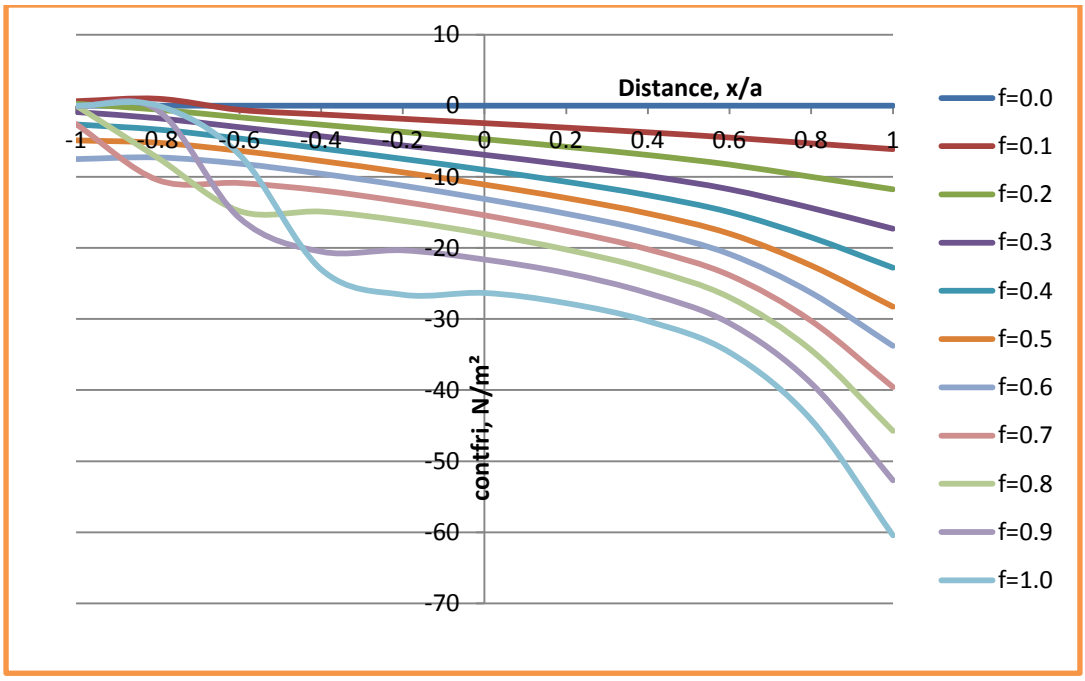

Figure 4.3: Distribution of contact frictional stress along the contact interface (*f*=0.1 to *f*=1.0)

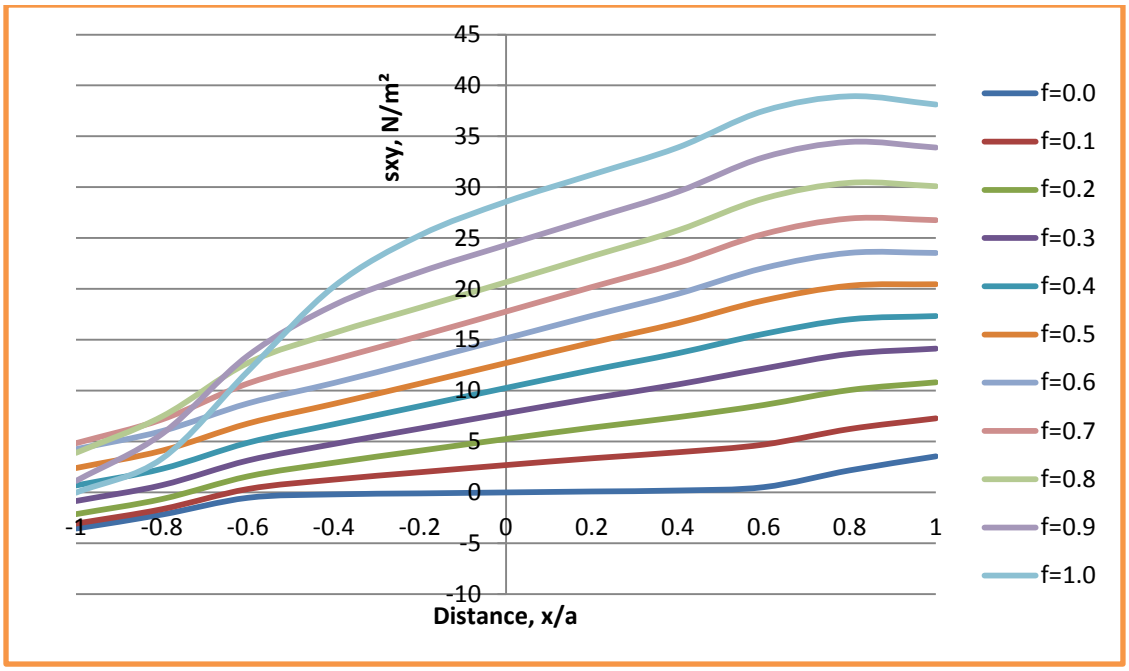

Figure 4.4: Distribution of contact shear stress, sxy along the contact interface (*f*=0.1 to *f*=1.0)

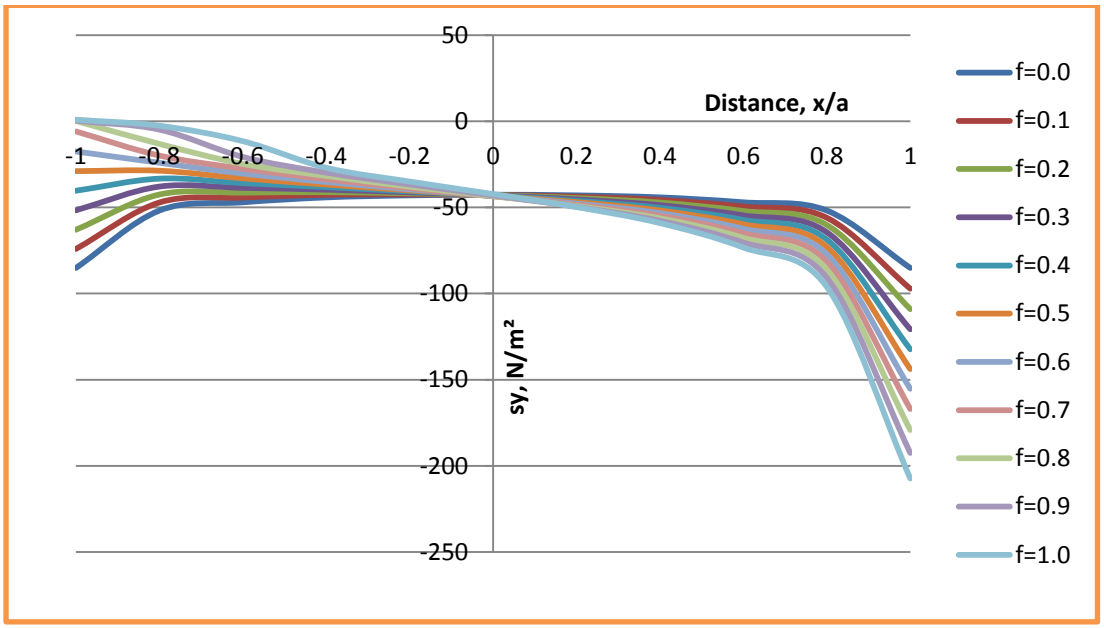

Figure 4.5: Distribution of contact normal stress, sy along the contact interface (*f*=0.1 to *f*=1.0)

Figure 4.1 shows the distribution of contact pressure along the contact interface, from f = 0.0 to f = 0.4. Meanwhile, Figure 4.2 shows the distribution of contact pressure along the contact interface, from f = 0.5 to f= 1.0. From these two figures, it is clear that at the trailing edge of the contact, the contact pressure decreases when f is greater. That means, the trailing edge of the punch is slightly lifted resulting in an incomplete contact between the punch and the half-plane.

Figure 4.3 shows the distribution of contact frictional stress along the contact interface, from f = 0.0 to f = 1.0. The value of compressive stress at the leading edge increases with greater f. This is simply because the shearing force on the punch increases as f increases, making the punch to create greater pressure at leading edge.

Figure 4.4 shows the distribution of contact shear stress along the contact interface, from f = 0.0 to f = 1.0. Figure 4.5 shows the distribution of contact normal stress along the contact interface, from f = 0.0 to f = 1.0. Referring to both figures, at the leading edge, the stress value increases along with f, neglecting the sign (negative sign shows the opposite direction). This is because when greater shearing force is applied to the punch, the leading edge of the punch will move slightly downwards, creating greater pressure with half-plane.

4.2 Subsurface stress analysis

For the subsurface stress analysis, only normal stress and shear stress will be shown. Contour plot is the most common medium to show the stress distribution in the subsurface.

For *f*=0.2,

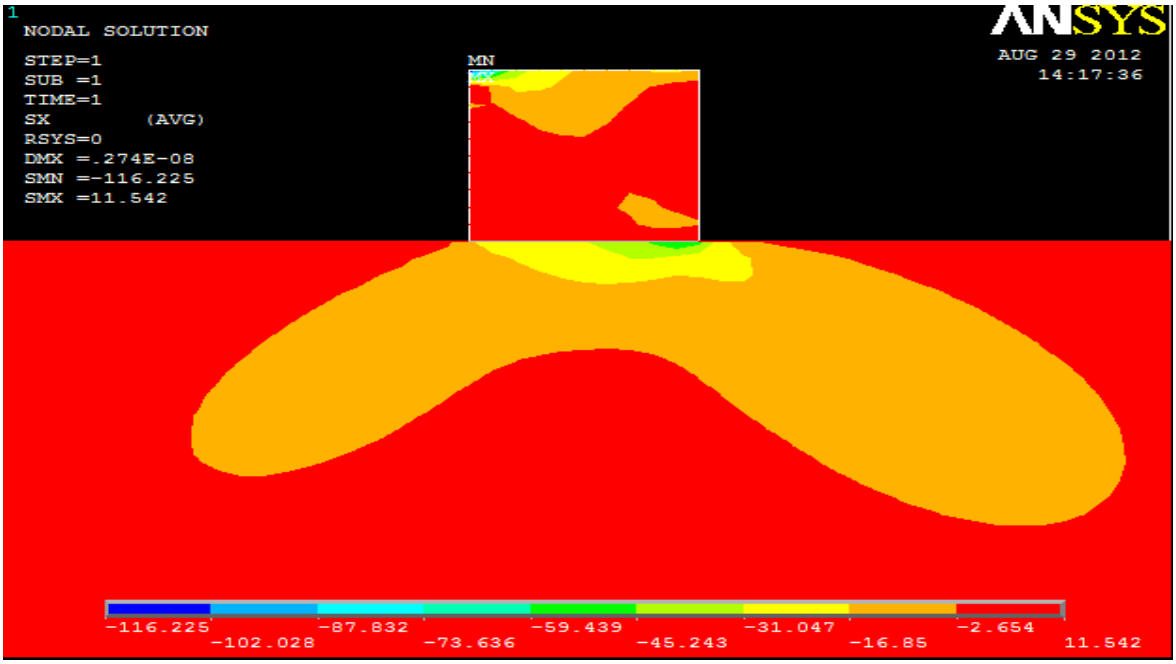

Figure 4.6: Contour plot of normal stress distribution in X-direction (*f*=0.2)

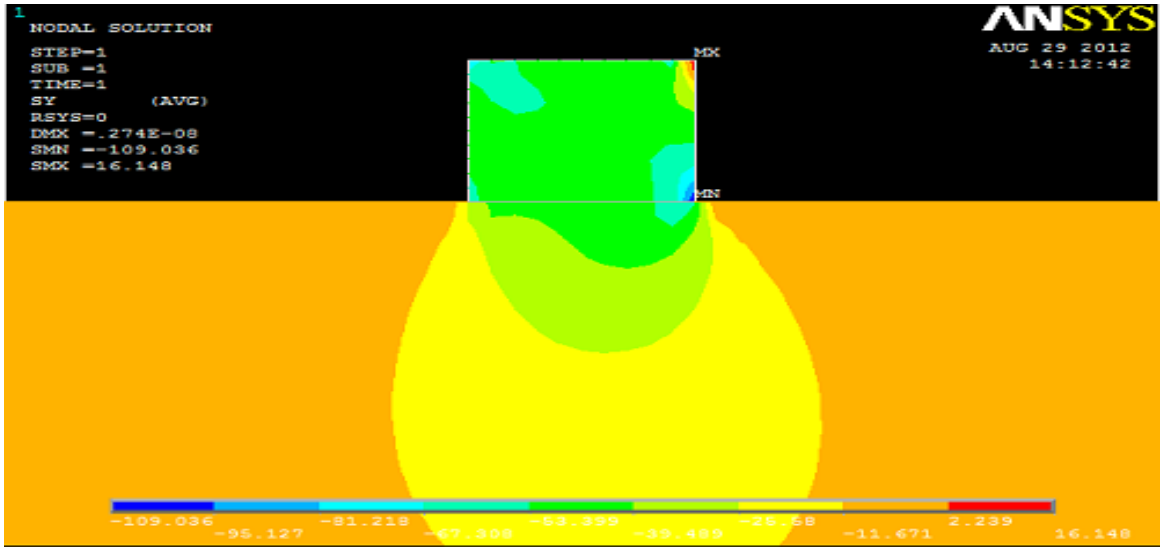

Figure 4.7: Contour plot of normal stress distribution in Y-direction (*f*=0.2)

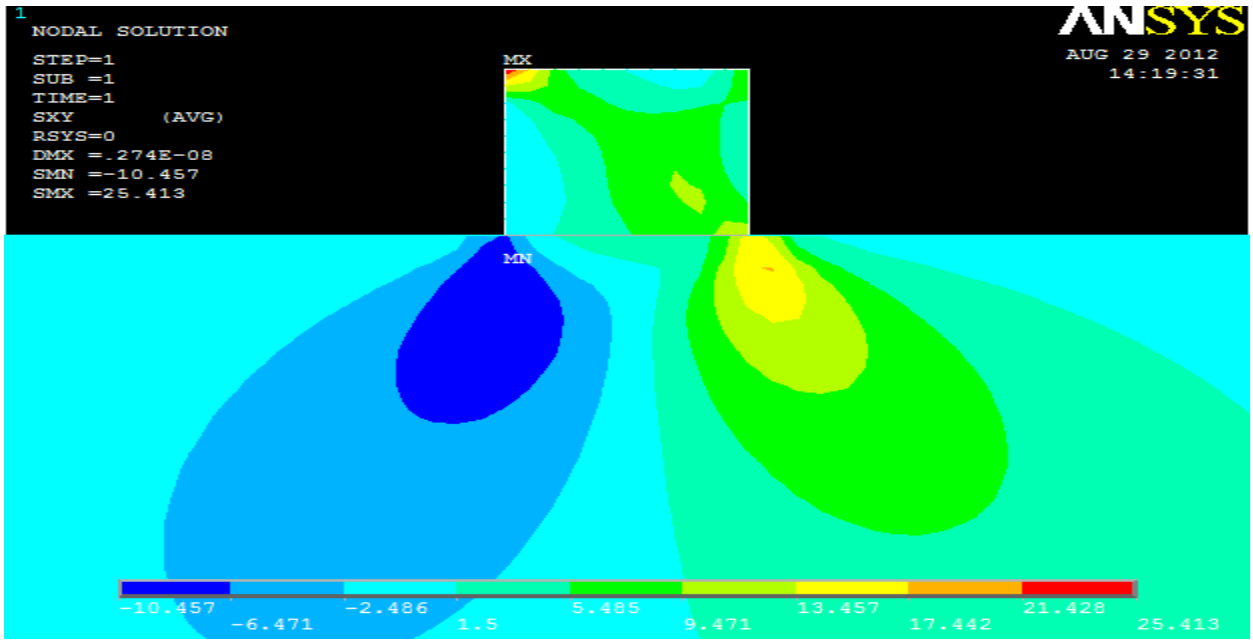

Figure 4.8: Contour plot of shear stress distribution in XY-direction (*f*=0.2)

For *f*=0.4

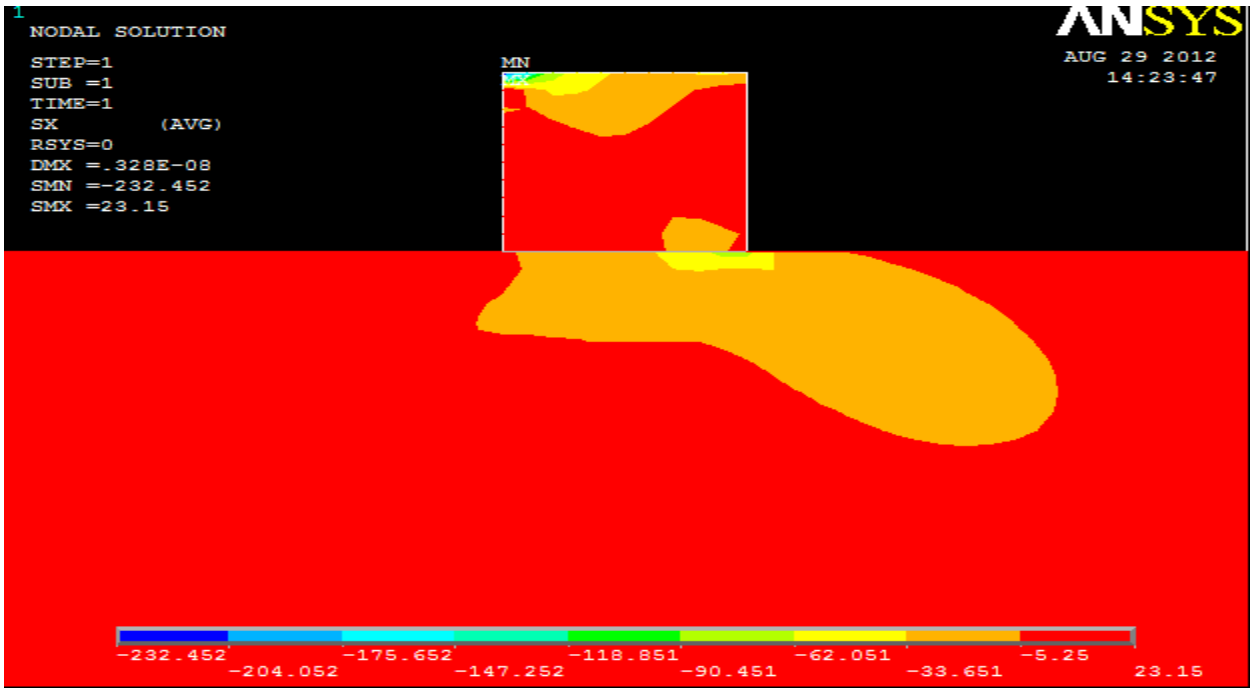

Figure 4.9: Contour plot of normal stress distribution in X-direction (*f*=0.4)

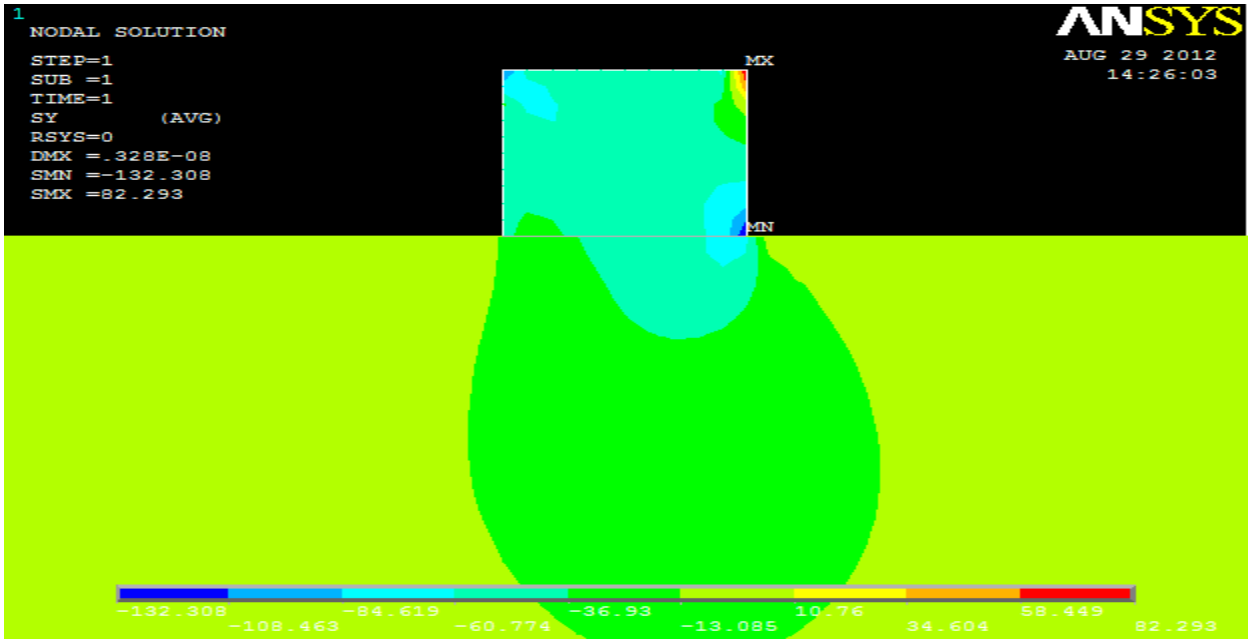

Figure 4.10: Contour plot of normal stress distribution in Y-direction (*f*=0.4)

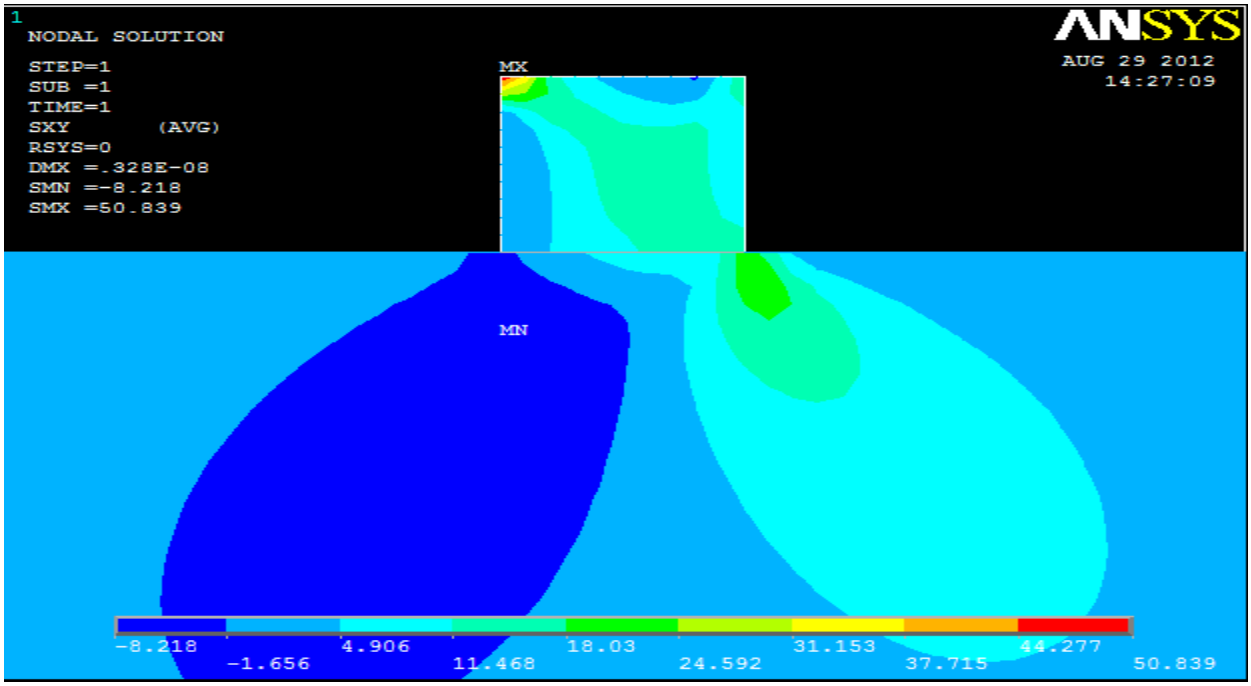

Figure 4.11: Contour plot of shear stress distribution in XY-direction (*f*=0.4)

For *f*=0.6

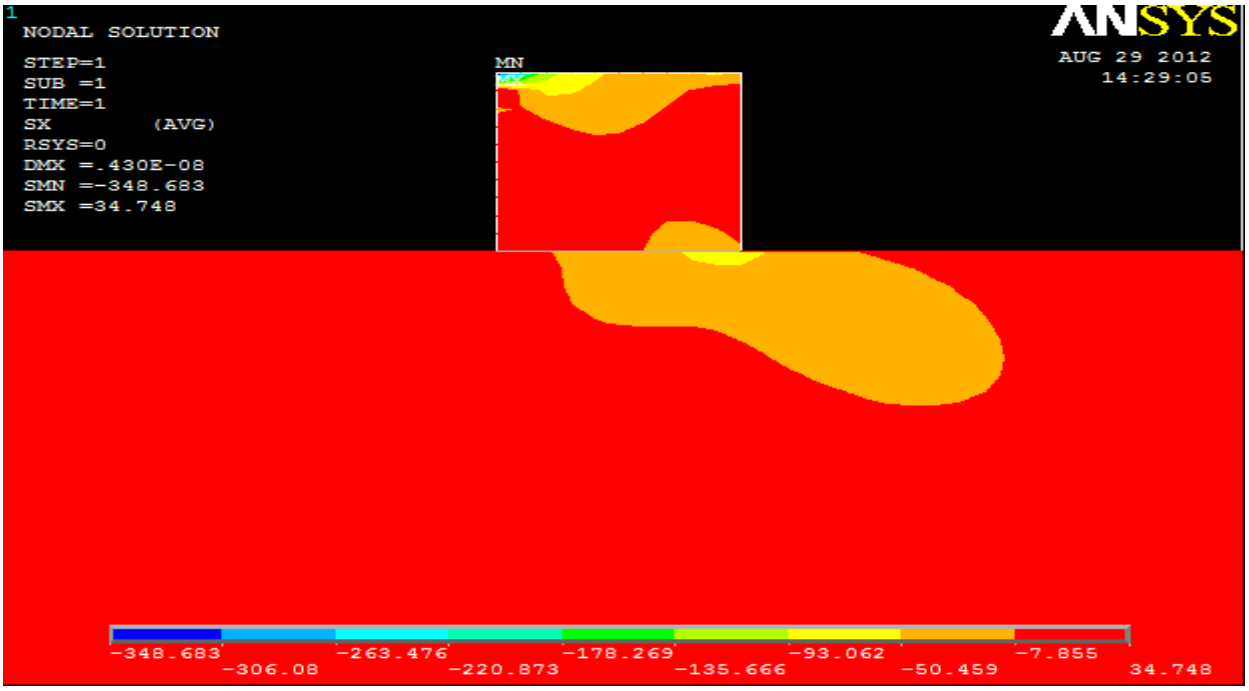

Figure 4.12: Contour plot of normal stress distribution in X-direction (*f*=0.6)

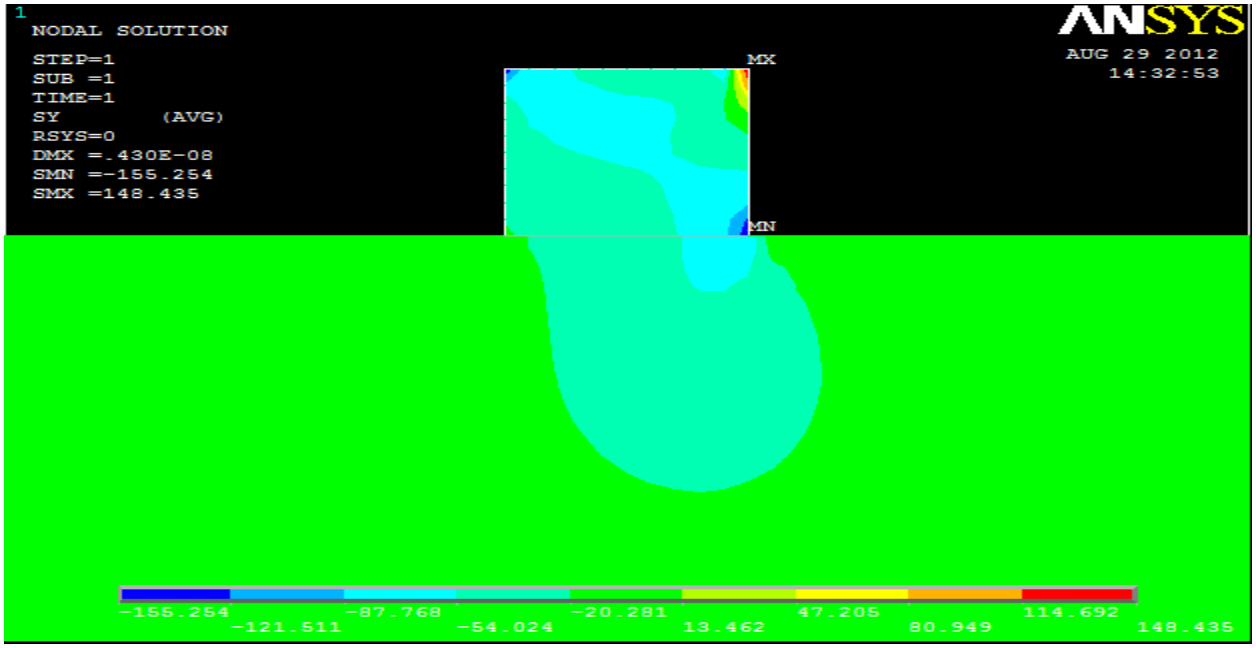

Figure 4.13: Contour plot of normal stress distribution in Y-direction (*f*=0.6)

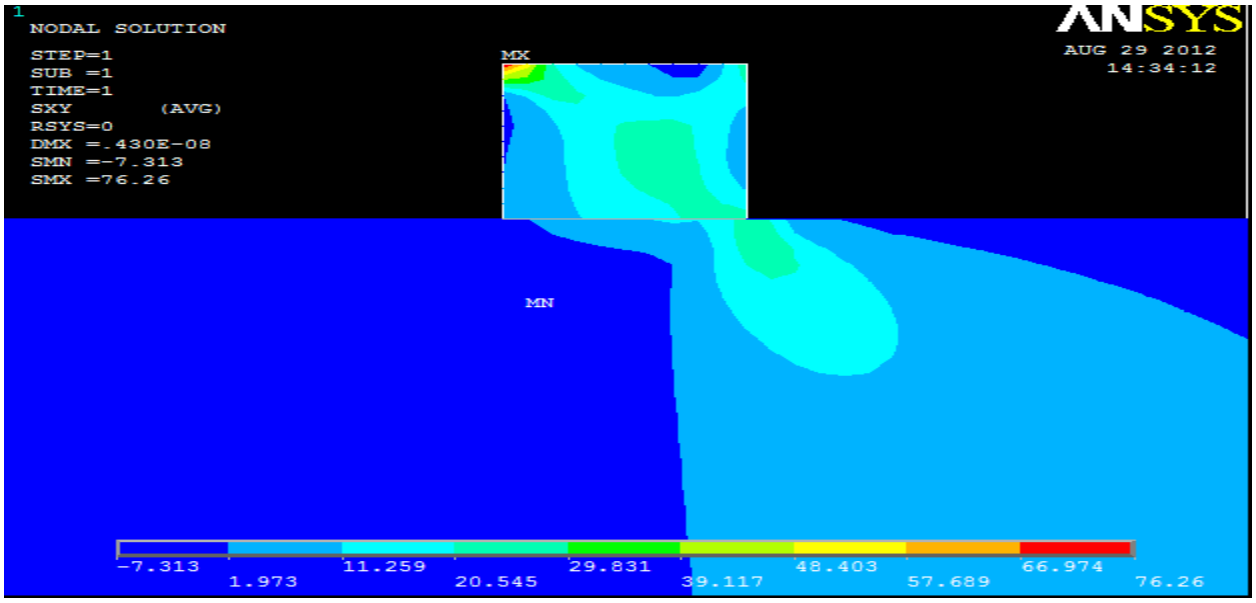

Figure 4.14: Contour plot of shear stress distribution in XY-direction (*f*=0.6)

For *f*=0.8,

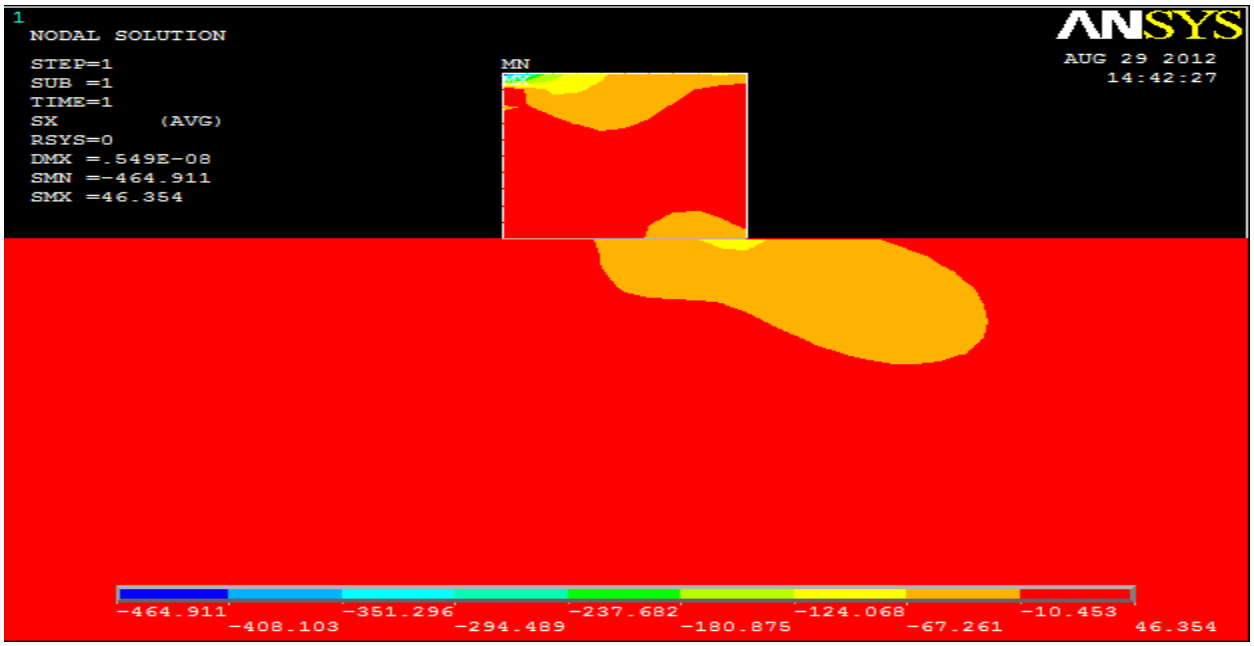

Figure 4.15: Contour plot of normal stress distribution in X-direction (*f*=0.8)

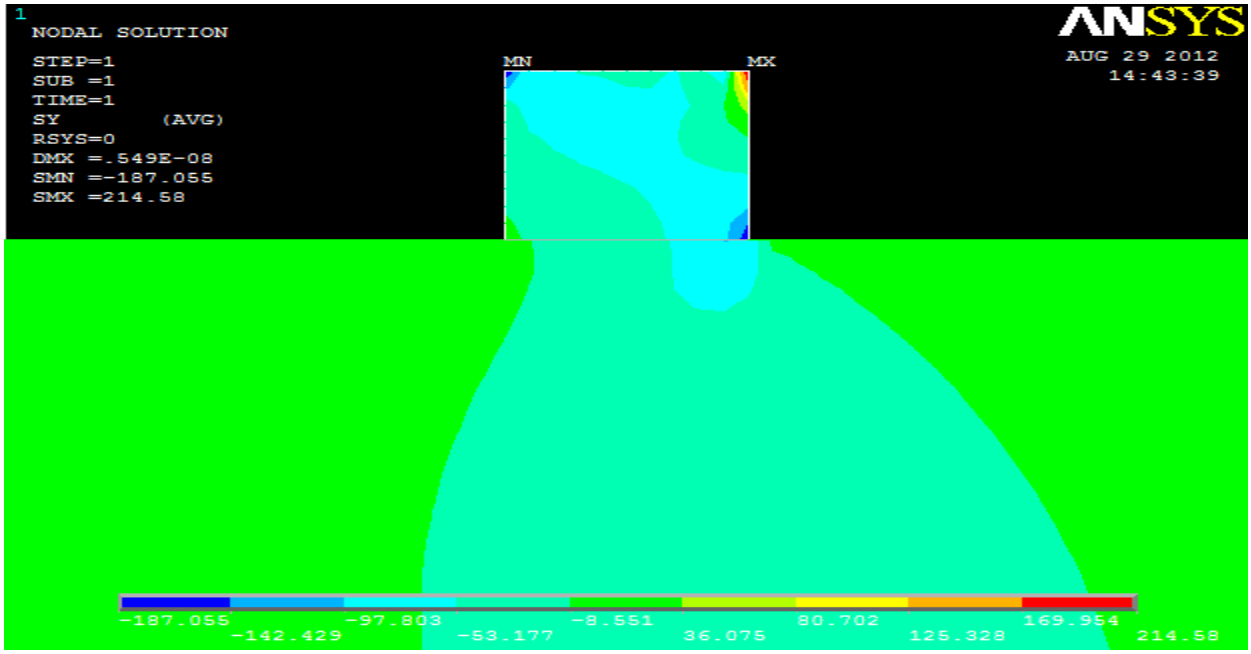

Figure 4.16: Contour plot of normal stress distribution in Y-direction (*f*=0.8)

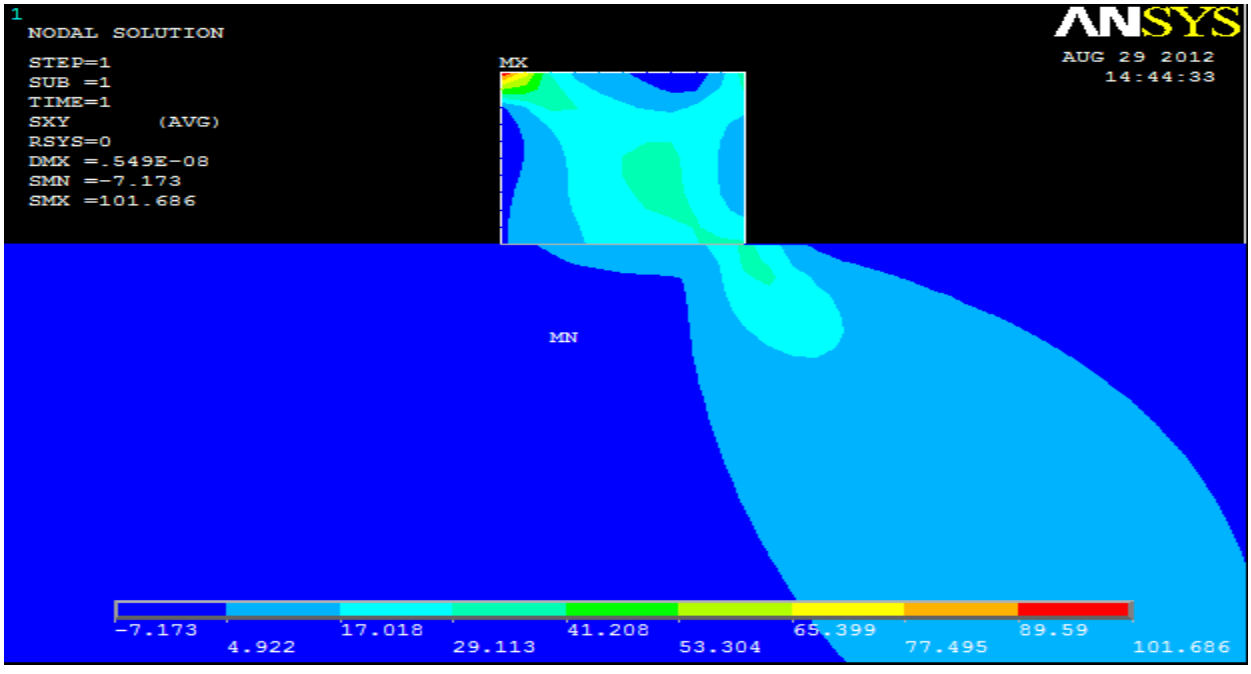

Figure 4.17: Contour plot of shear stress distribution in XY-direction (*f*=0.8)

For *f*=1.0

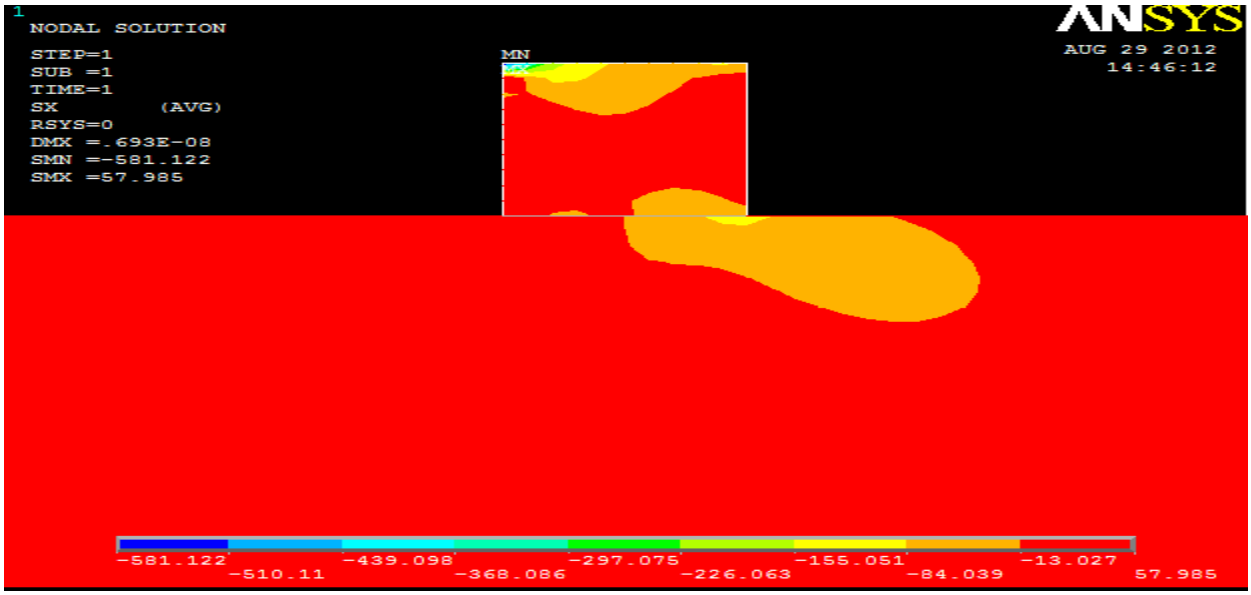

Figure 4.18: Contour plot of normal stress distribution in X-direction (*f*=1.0)

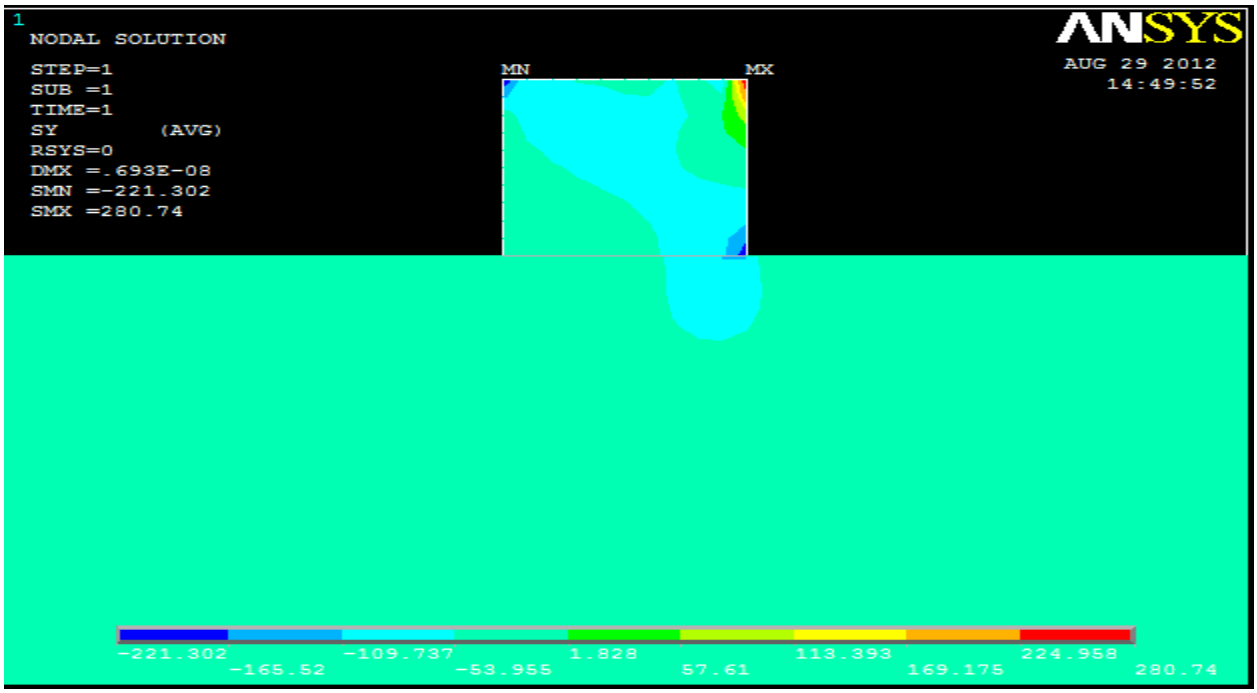

Figure 4.19: Contour plot of normal stress distribution in Y-direction (*f*=1.0)

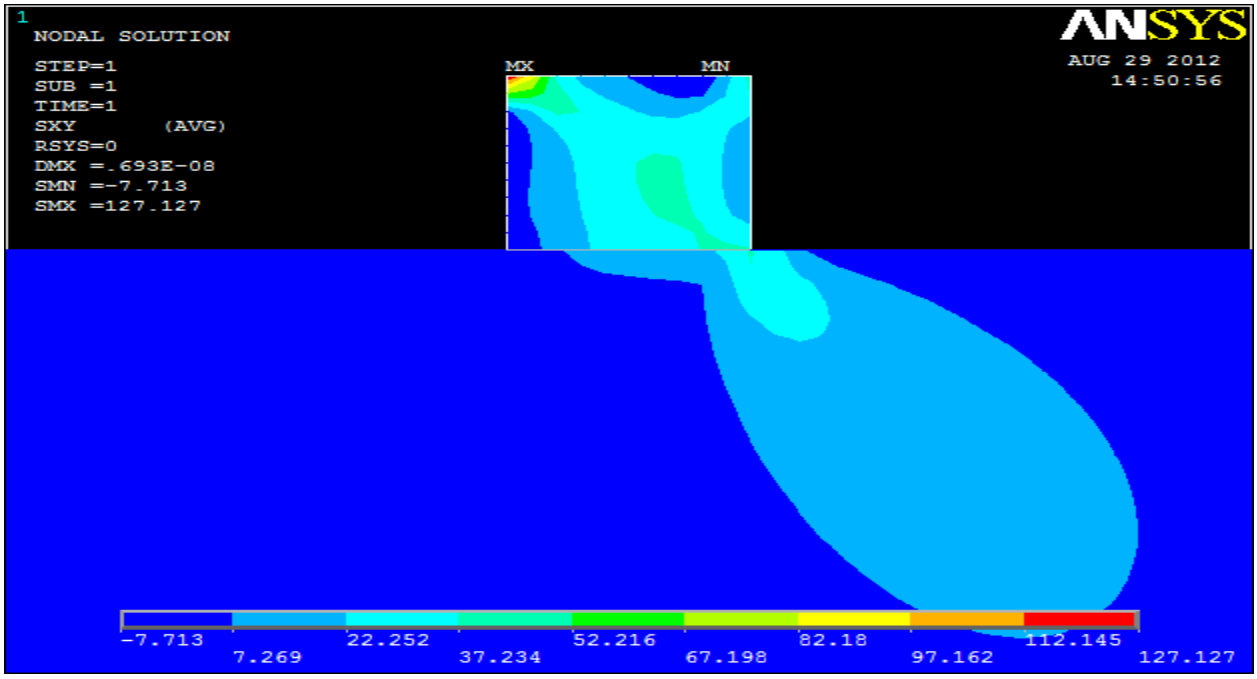

Figure 4.20: Contour plot of shear stress distribution in XY-direction (*f*=1.0)

Figure 4.6 until Figure 4.20 shows the contour plots of normal stress in X-direction, Y-direction, and shear stress in XY-direction, when f = 0.2, 0.4, 0.6, 0.8 and 1.0.

To analyze the subsurface even better, the author had refined the mesh at both trailing and leading edge to 0.04 m. Then, stress values of normal stress in X-direction, normal stress in Y-direction and shear stress in XY-direction were transferred to Microsoft Excel to create contours of these stresses when f = 0.2, 0.4 and 0.8.

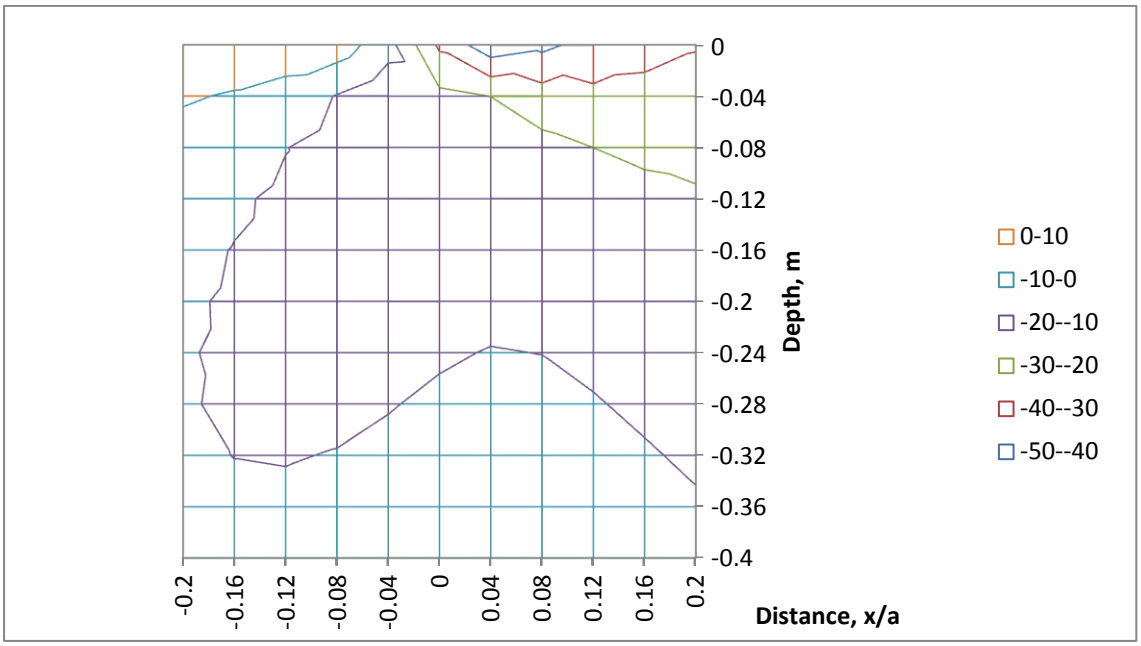

Figure 4.21: Contour of subsurface normal stress in X-direction at trailing edge, *f* = 0.2

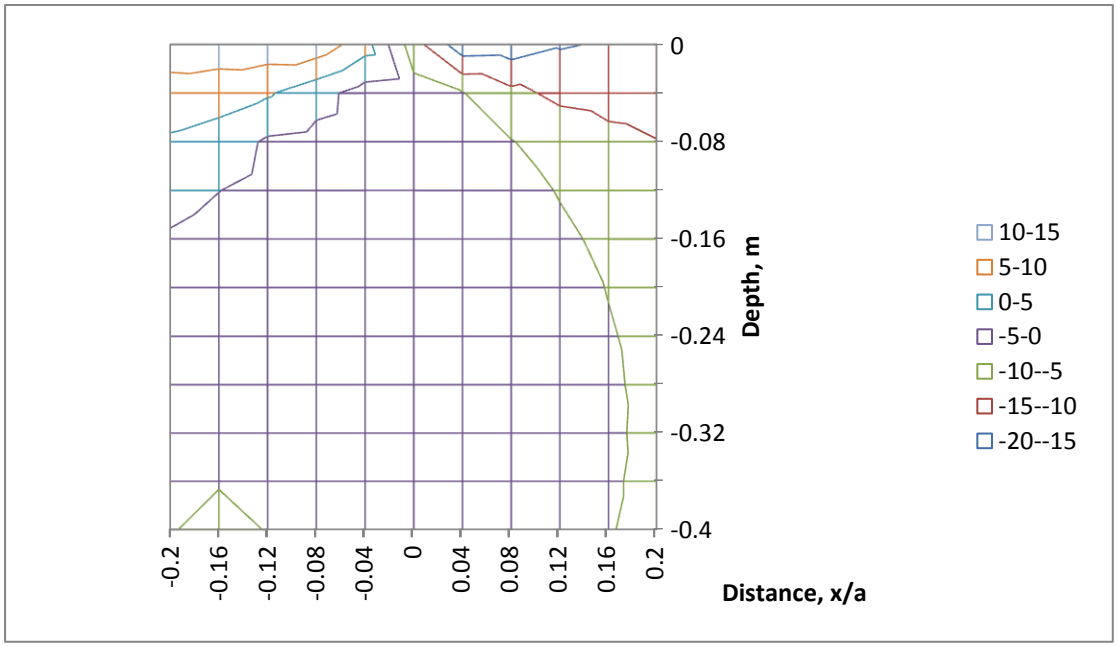

Figure 4.22: Contour of subsurface normal stress in X-direction at trailing edge, *f* = 0.4

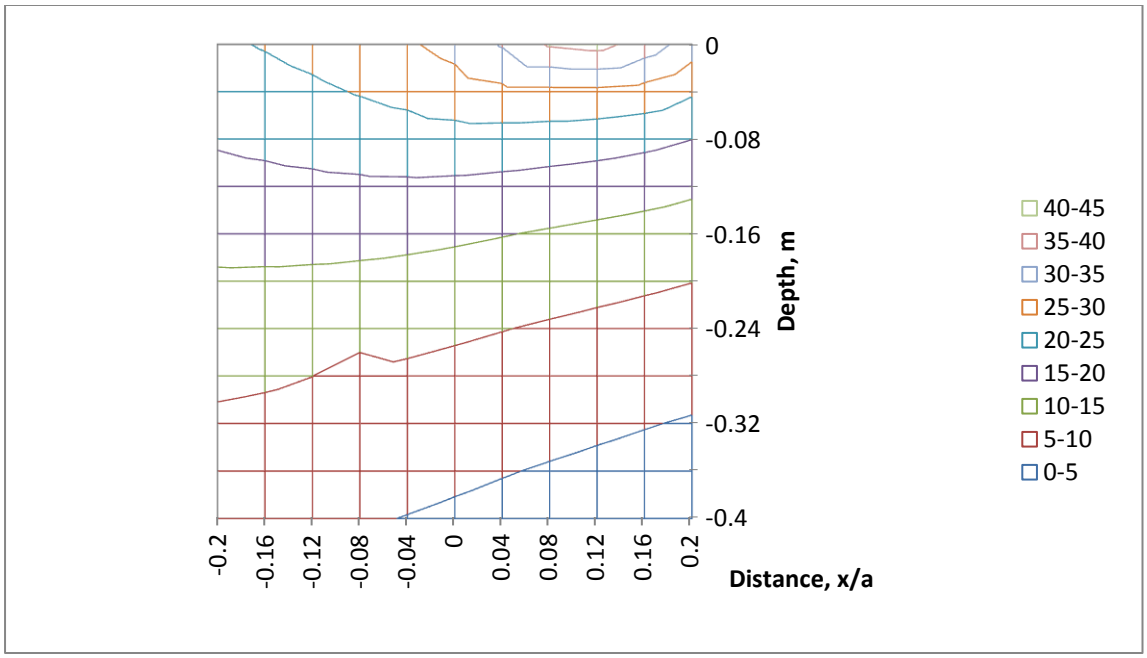

Figure 4.23: Contour of subsurface normal stress in X-direction at trailing edge, *f* = 0.8

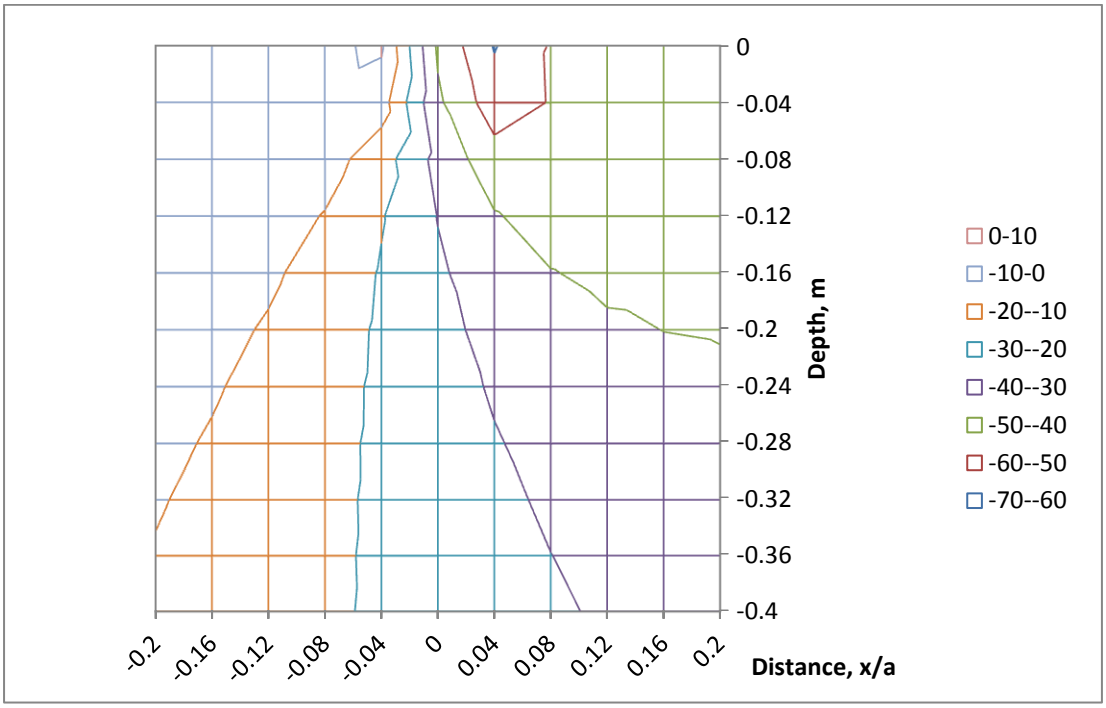

Figure 4.24: Contour of subsurface normal stress in Y-direction at trailing edge, *f* = 0.2

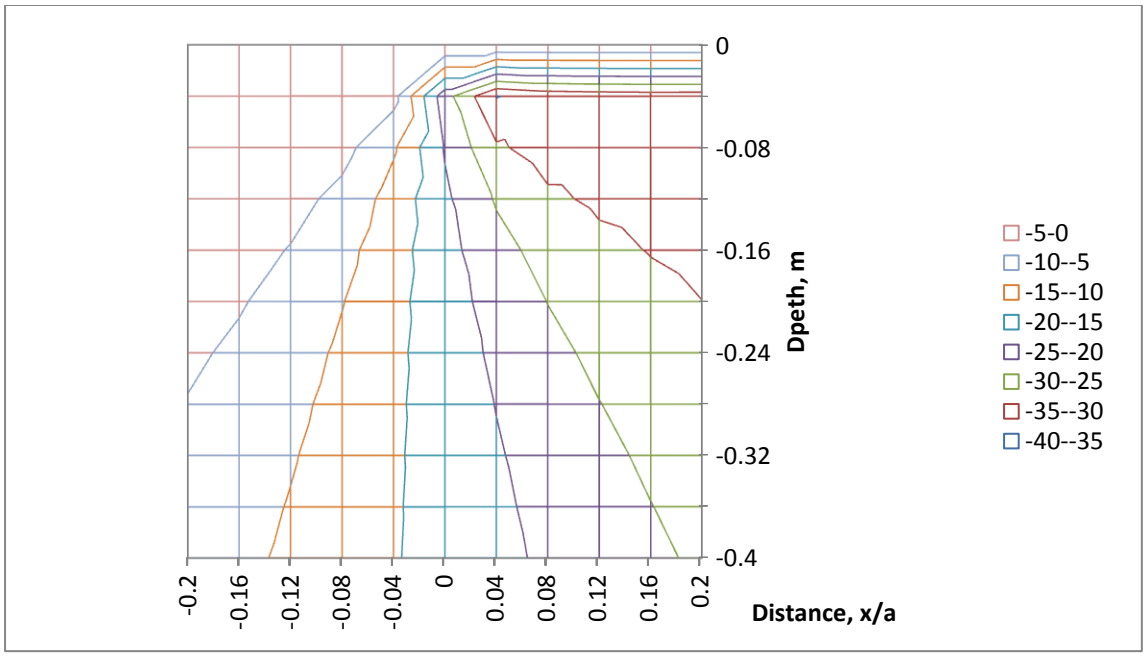

Figure 4.25: Contour of subsurface normal stress in Y-direction at trailing edge, *f* = 0.4

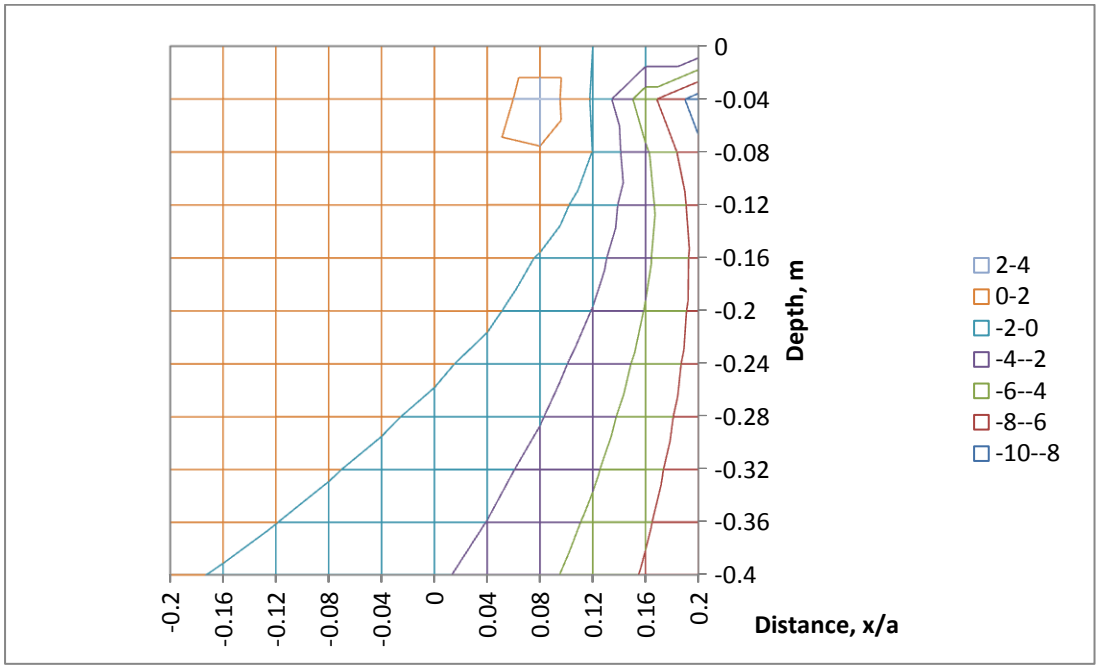

Figure 4.26: Contour of subsurface normal stress in Y-direction at trailing edge, *f* = 0.8

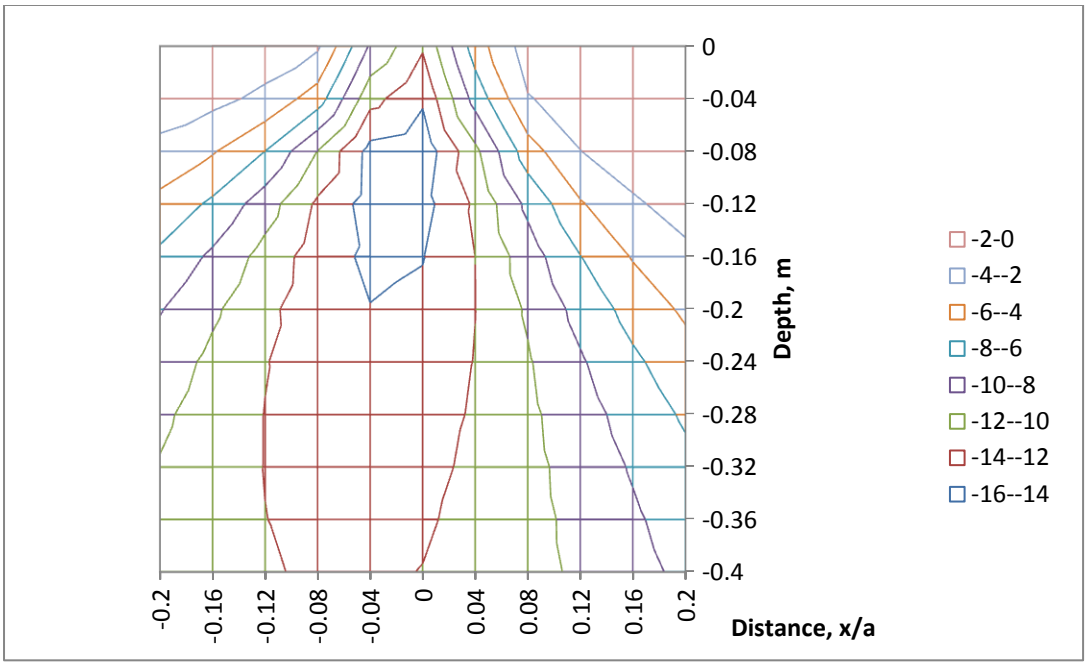

Figure 4.27: Contour of subsurface shear stress in XY-direction at trailing edge, *f* = 0.2

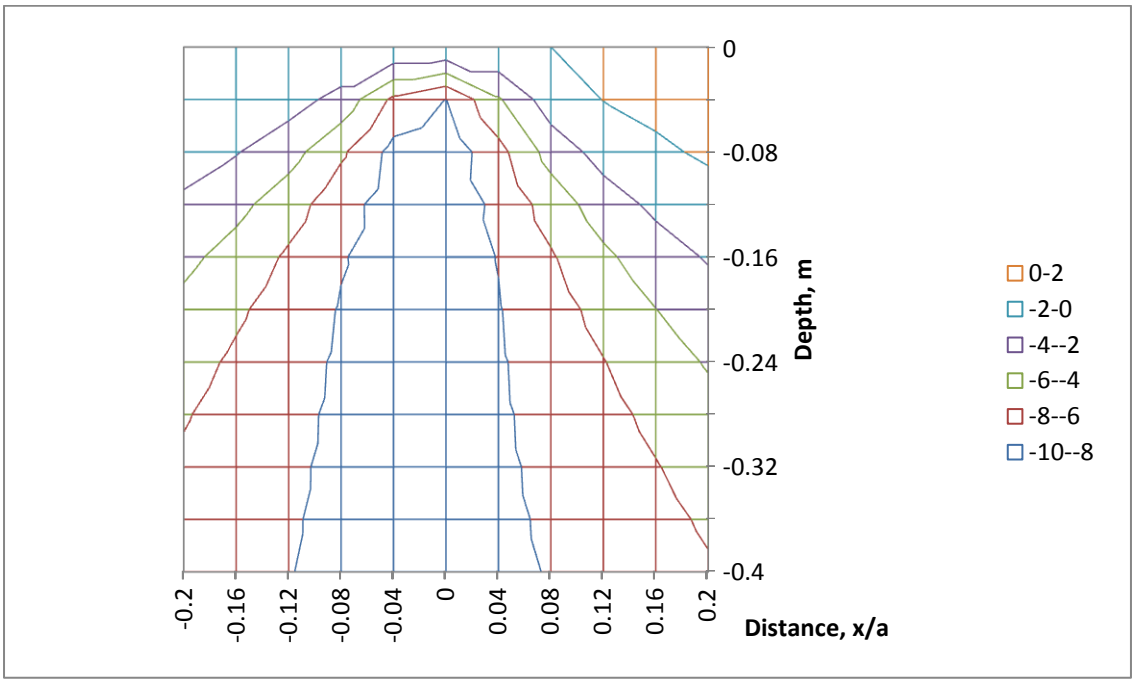

Figure 4.28: Contour of subsurface shear stress in XY-direction at trailing edge, *f* = 0.4

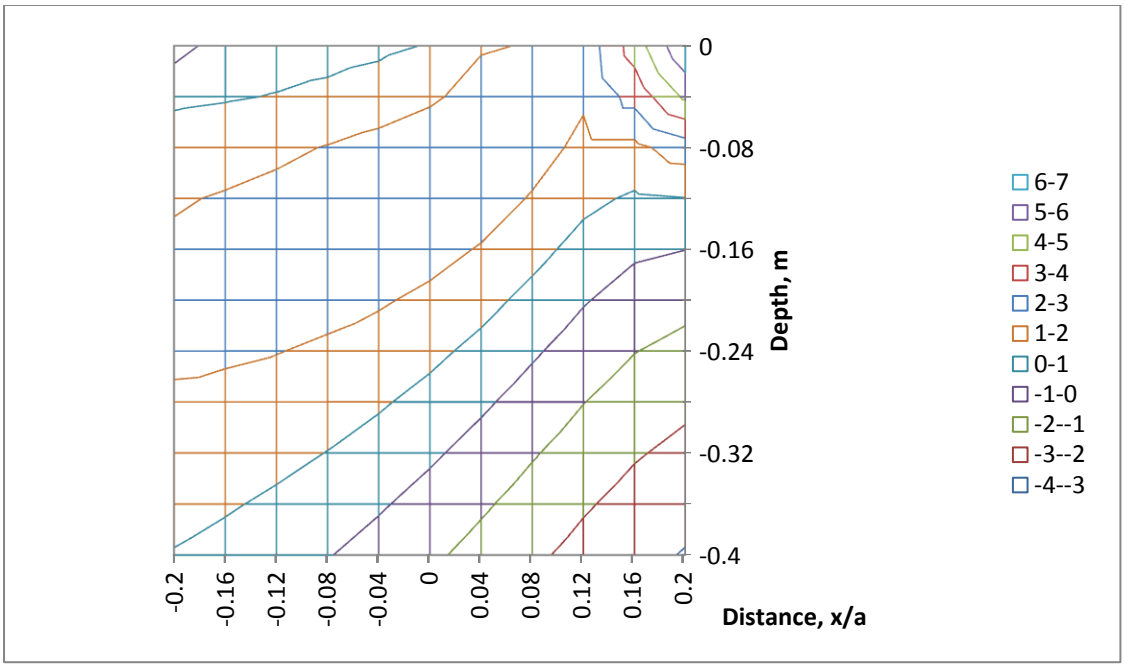

Figure 4.29: Contour of subsurface shear stress in XY-direction at trailing edge, *f* = 0.8

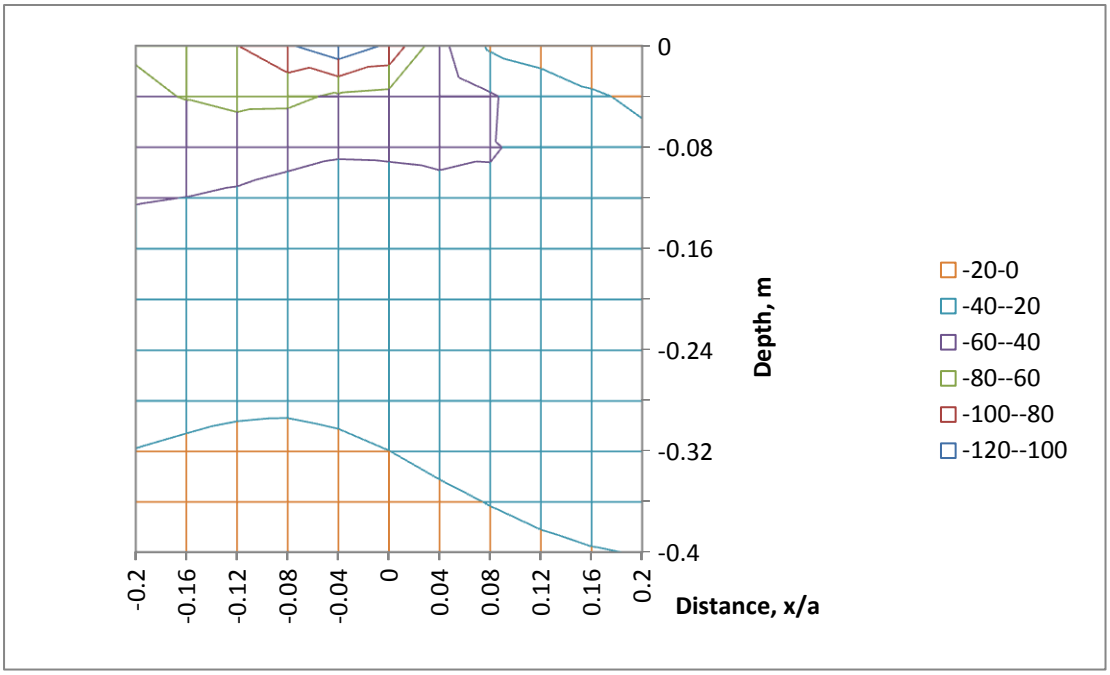

Figure 4.30: Contour of subsurface normal stress in X-direction at leading edge, *f* = 0.2

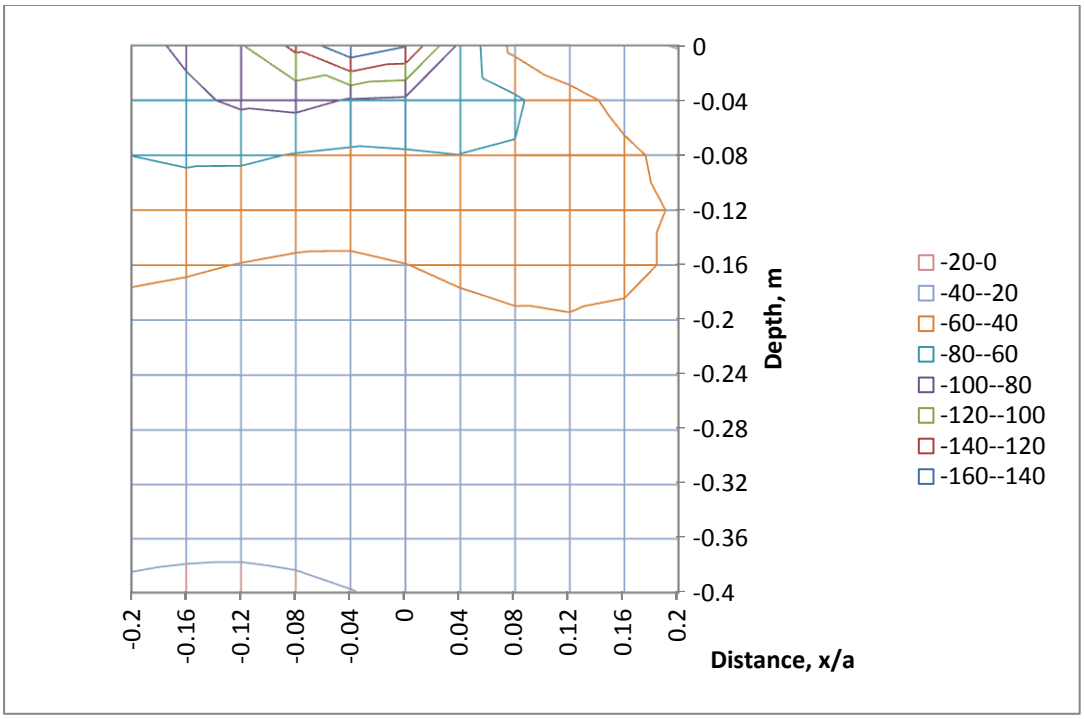

Figure 4.31: Contour of subsurface normal stress in X-direction at leading edge, *f* = 0.4

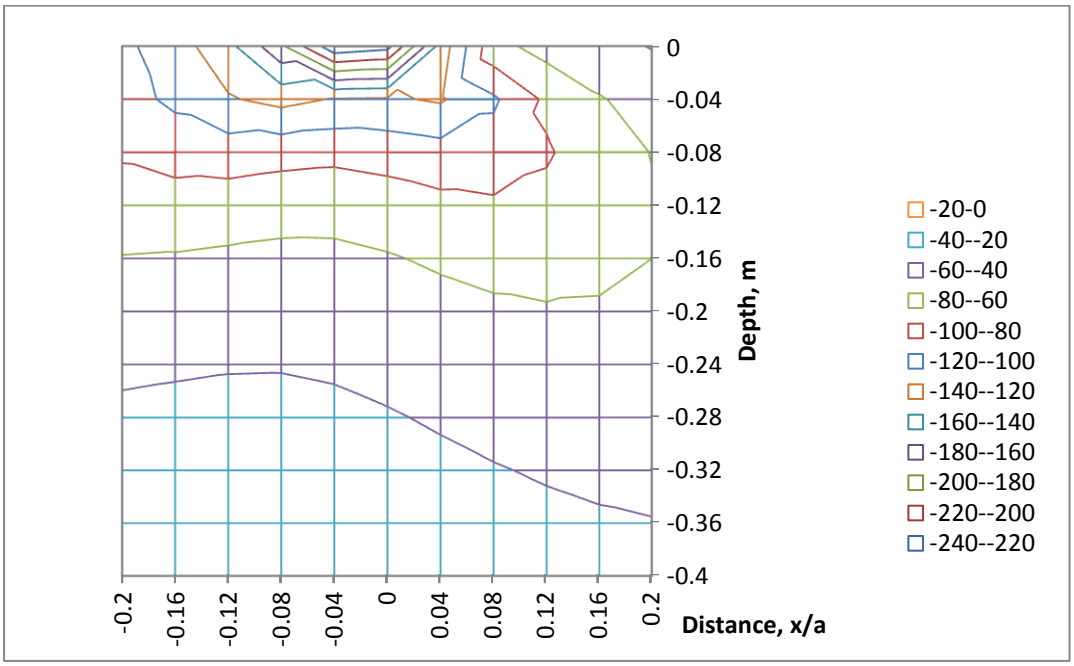

Figure 4.32: Contour of subsurface normal stress in X-direction at leading edge, *f* = 0.8

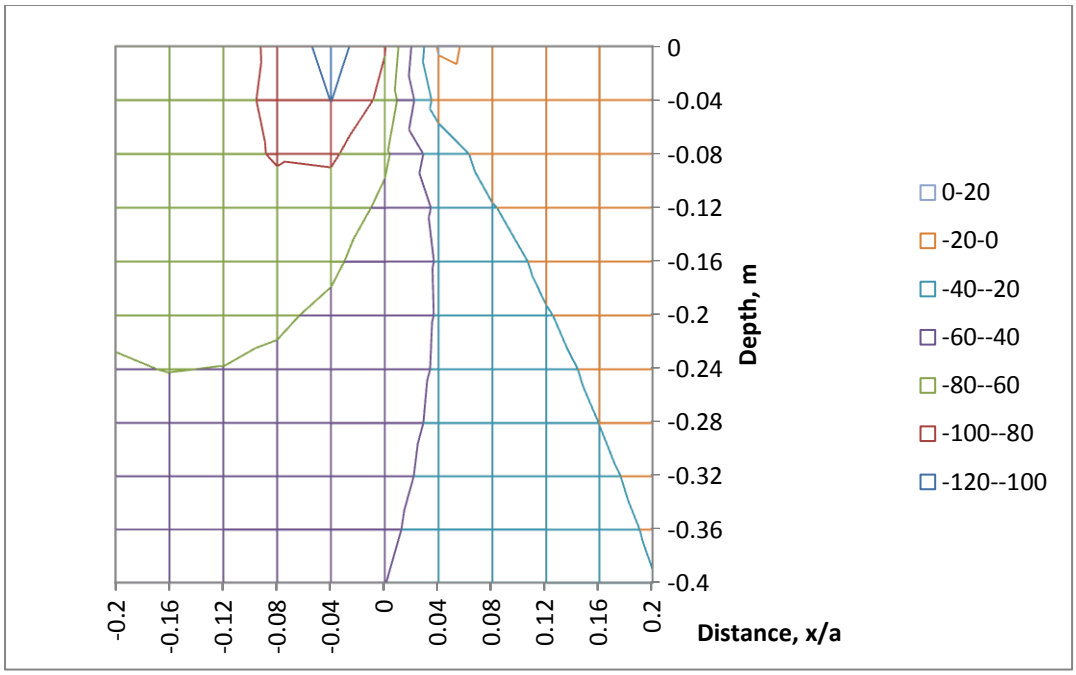

Figure 4.33: Contour of subsurface normal stress in Y-direction at leading edge, *f* = 0.2

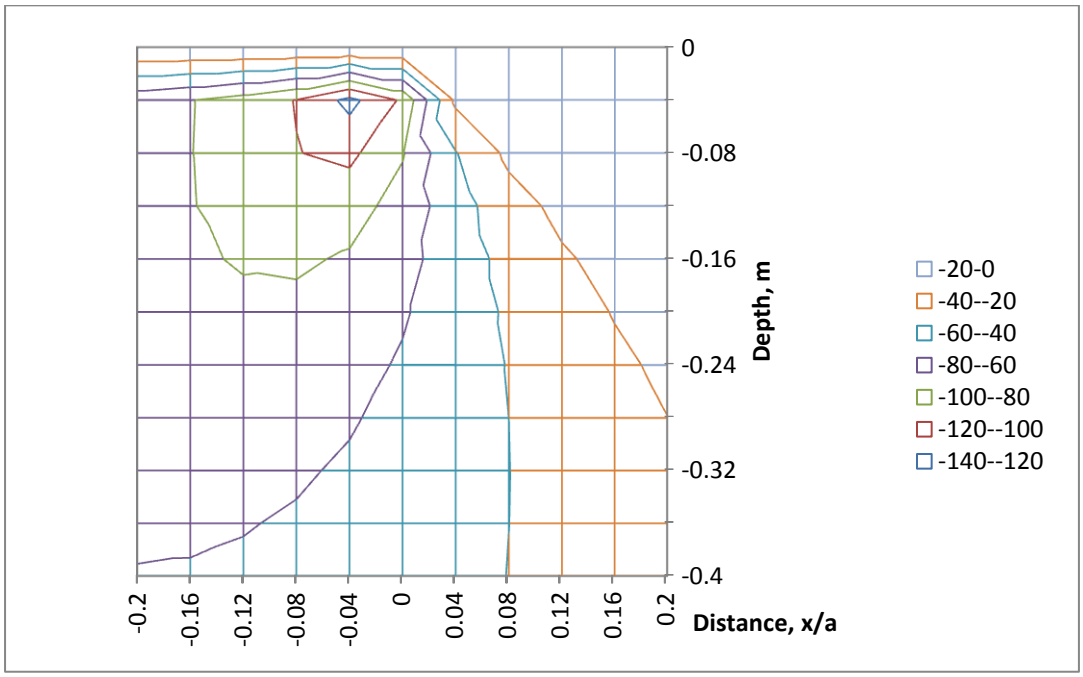

Figure 4.34: Contour of subsurface normal stress in Y-direction at leading edge, *f* = 0.4

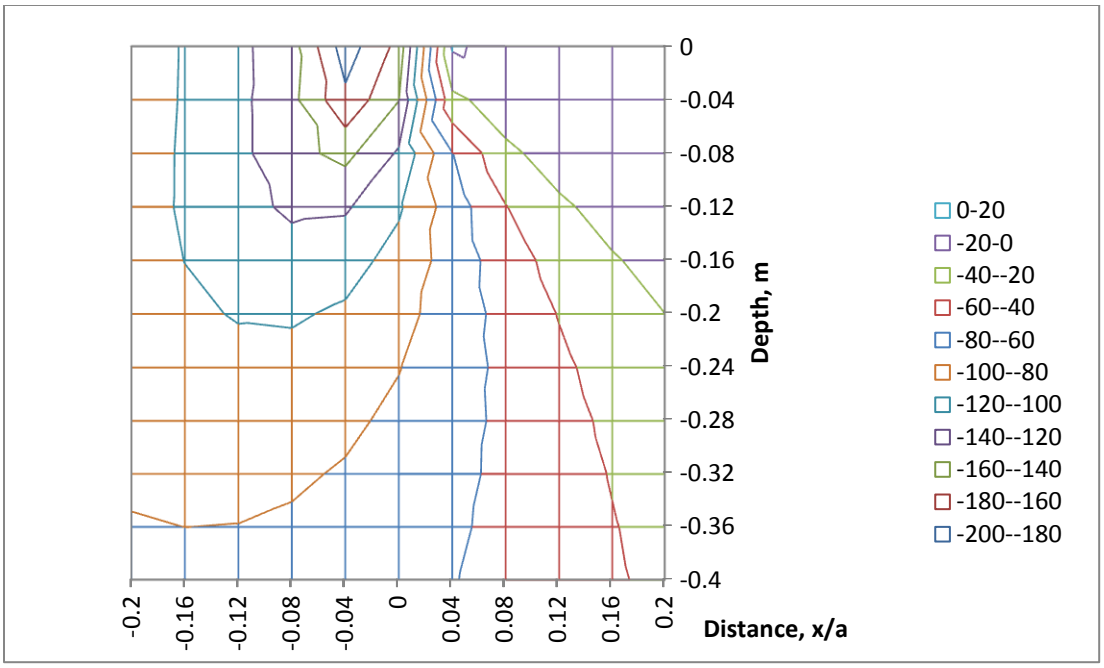

Figure 4.35: Contour of subsurface normal stress in Y-direction at leading edge, *f* = 0.8

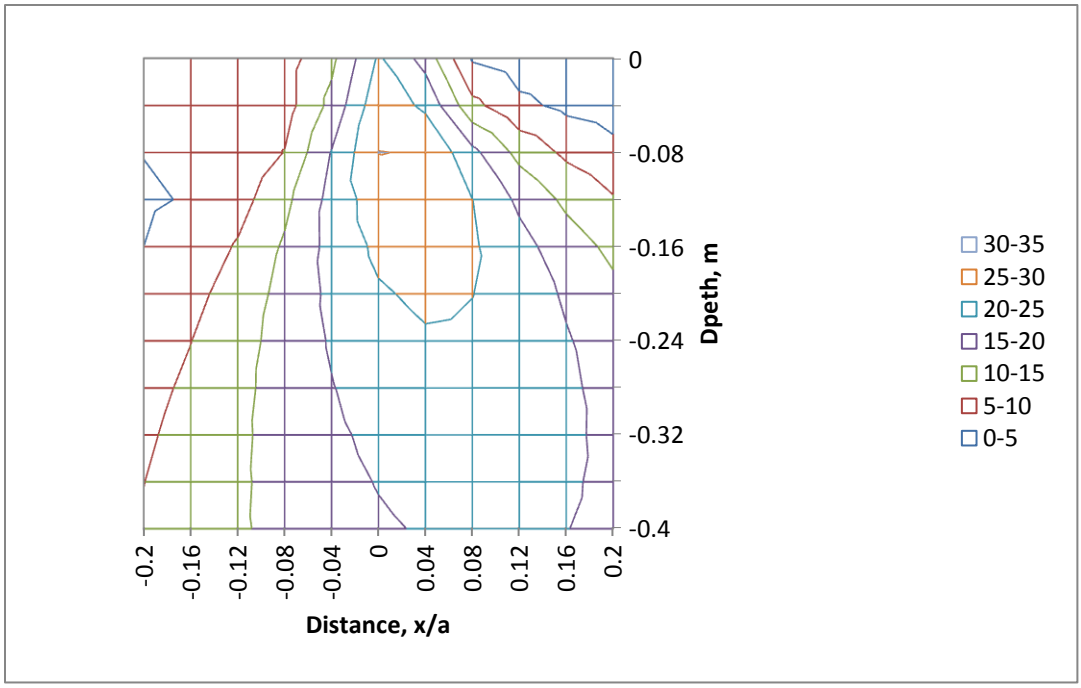

Figure 4.36: Contour of subsurface shear stress in XY-direction at leading edge, *f* = 0.2

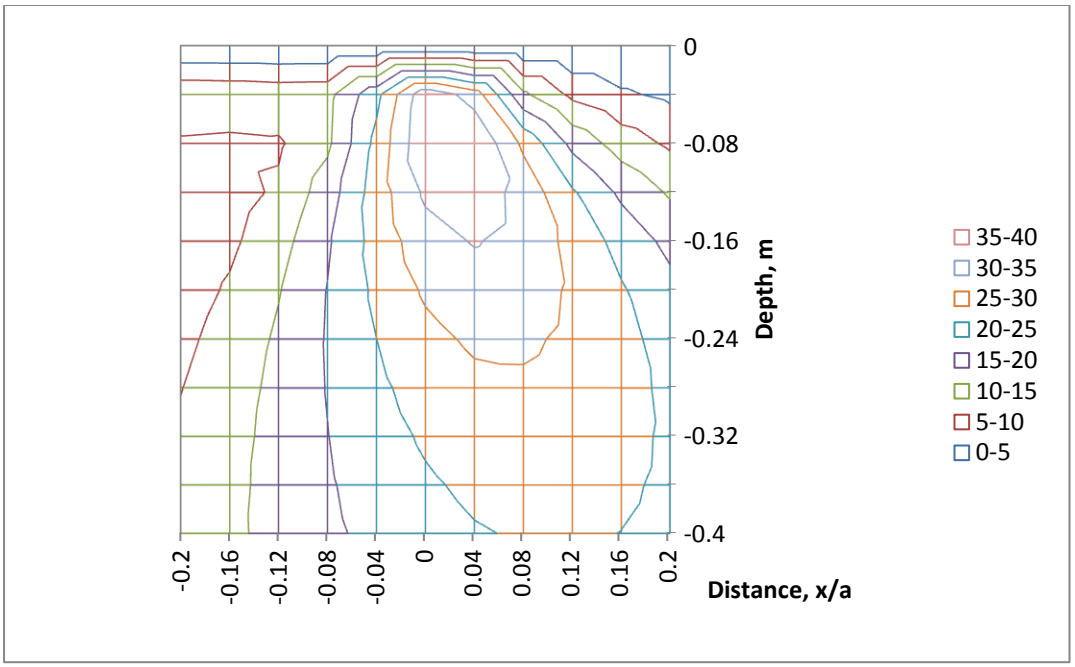

Figure 4.37: Contour of subsurface shear stress in XY-direction at leading edge, *f* = 0.4

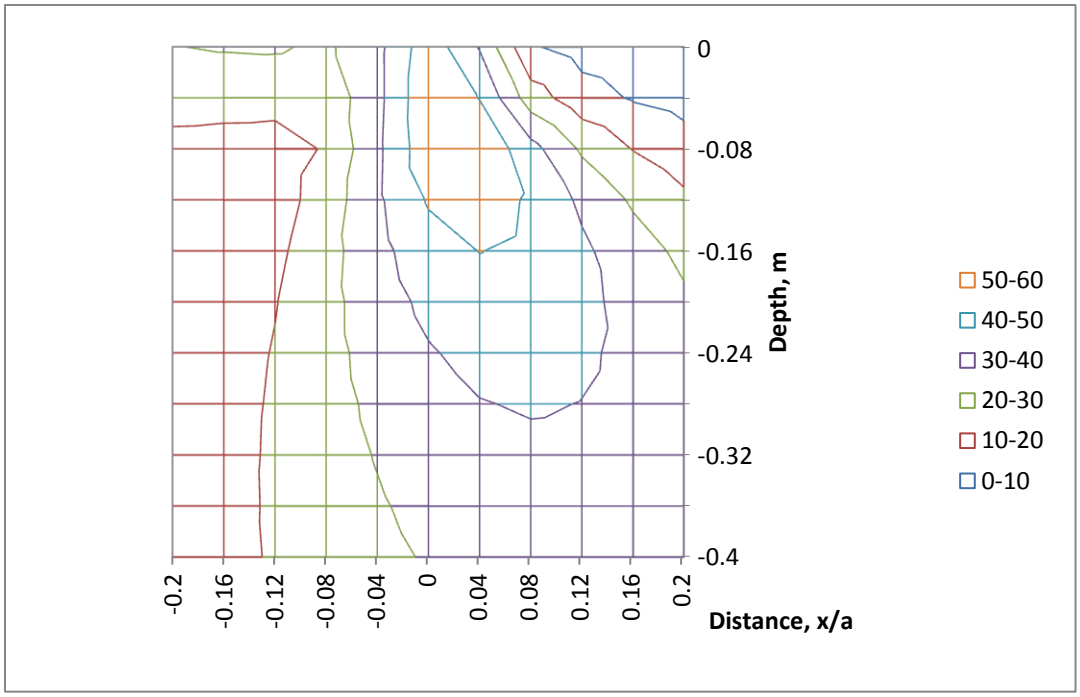

Figure 4.38: Contour of subsurface shear stress in XY-direction at leading edge, *f* = 0.8

Figure 4.21 to Figure 4.38 show the contour plot of the distribution of normal stress in X-direction and Y-direction, and shear stress in XY-direction when f = 0.2, 0.4 and 0.8, at trailing and leading edge. The trailing or leading edge of the punch lies on the coordinate (0,0) on each figure. For trailing edge, the contact interface between the punch and half-plane is from (0,0) until (0.2,0). Meanwhile, for leading edge, the contact interface is from (-0.2,0) until (0,0).

Based on Figure 4.21 to Figure 4.23, the changes of stress on the top of the half-plane are quite obvious. When f = 0.2, the right side of the contour (just below the contact interface) is having compressive stress, and the left side experience tensile stress (positive value of stress). As f increases, it is clear that the compressive stress decreases, and the tensile stress increases. This is simply because the punch is not fully in contact with half-plane, and that will reduce the compressive normal stress at subsurface.

From Figure 4.30 to Figure 4.32, stress is highly concentrated at the left side (just below the contact interface). As f increases, the stress at that area increases as well. This is because shearing force is greater. That is the most critical area of the contact, which experience higher stress than other areas.

CHAPTER 5

CONCLUSION / RECOMMENDATION

5.1 Conclusion

Based on the results obtained from simulation using ANSYS, it is clear that contact pressure at both trailing and leading edge is the highest compared to any other areas after applying pressure on top of the punch. But after applying shearing force and other forces to balance the moment, the contact pressure at the trailing edge decreases, but at the leading edge, the contact pressure increases. The stress value at trailing edge is less than at the center of contact interface when f is equal and larger than 0.5. This is because the trailing edge of the punch is slightly lifted, forming a gap between the punch and the half-plane. Thus, the contact pressure at trailing edge decreases as f increases.

After analyzing all the results, it can be concluded that the stress at leading edge is the greatest. In order to reduce the stress at this area, the pressure applied on top of the punch must be reduced. Other than that, shearing force also needs to be reduced. Leading edge of the punch is the most critical area of sliding contact, which may lead to a component's defect. Lower coefficient of friction, f will also reduce the stress at leading edge. In real life, there are many solutions to reduce the friction, for example, using lubricants such as oil or grease.

For subsurface stress analysis, it is confirmed that as f gets higher, the stress at leading edge increases, and stress at trailing edge decreases. This is due to the tendency of the punch to tilt, producing a small gap between trailing edge of the punch and the half-plane.

5.2 Recommendation

To obtain better results, it is recommended to perform both finite element analysis, which is done with ANSYS, and also analytical method [3]. This is to ensure the modeling and simulation using ANSYS are correct, and the results from the software are accurate.

Furthermore, in order to produce more accurate results, mesh has to be refined at certain important areas, including trailing and leading edge, especially for subsurface stress analysis, so that the results will be more detailed.

REFERENCES

[1] Guler MA, Erdogen F. Contact mechanics of two deformable elastic solids with graded coatings. Mechanics of Material 2006;38:633-47

[2] Karuppanan S, Churchman CM, Hills DA, Giner E. Sliding frictional contact between a square block and an elastically similar half-plane. European Journal of Mechanics A-Solids 2008;27:443-59

[3] Karuppanan S, Hills DA. Sliding of general frictional complete contacts. International Journal of Mechanical Sciences 2008;50:1404-10

[4] Churchman, C.H, Hills DA, Mugadu A. Asymptotic results for slipping complete frictional contacts. European Journal of Mechanics A/Solids 2003;22:793-800

[5] Mugadu A, Hills DA, Limmer L. An asymptotic approach to crack initiation in fretting fatigue of complete contacts. Journal of the Mechanics and Physics of Solids 2002;50:531-47

APPENDICES

Appendix A: Normalized contact pressure distribution along the contact surface [2][3]

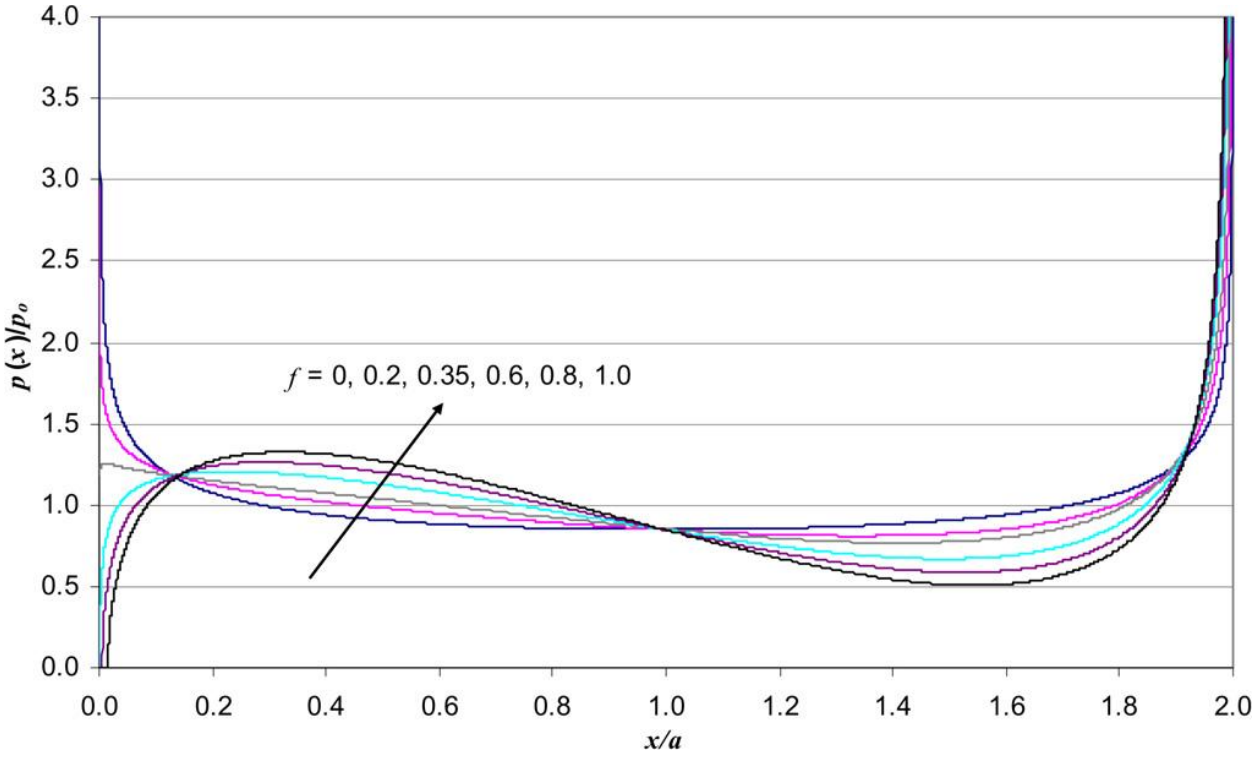

Appendix B: Normalized contact pressure distribution at the trailing edge [2][3]

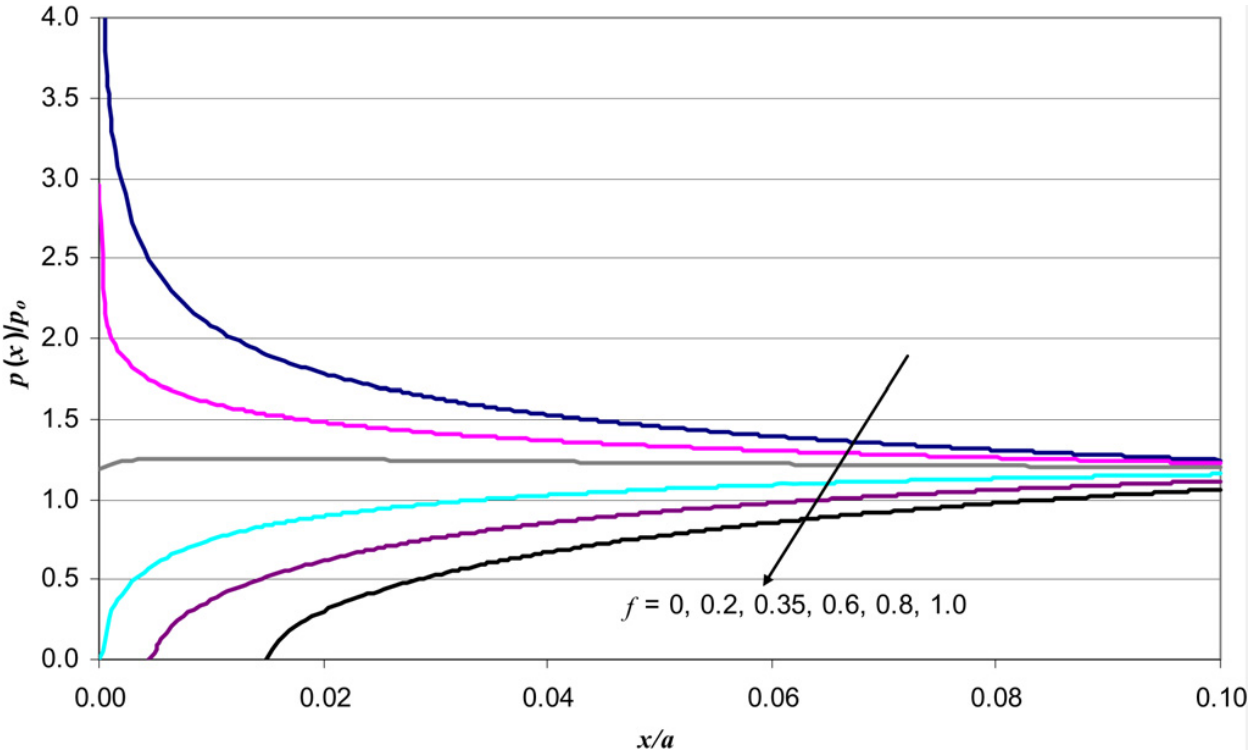

Appendix C: Normal stress in X-direction, N/m², at trailing edge, *f* = 0.2

6.7798	6.6085	6.2713	5.5483	-6.2678	-31.847	-46.433	-42.447	-36.104	-32.743	-30.492
0.98212	-0.85984	-3.9593	-10.516	-16.787	-17.676	-20.1	-25.726	-28.044	-27.623	-26.927
-3.6985	-6.2128	-9.7799	-13.072	-14.35	-14.464	-14.922	-16.99	-20.021	-21.959	-22.716
-6.8168	-9.0868	-11.298	-12.74	-13.041	-12.567	-12.505	-13.566	-15.453	-17.437	-18.907
-8.5857	-10.198	-11.477	-12.091	-11.958	-11.472	-11.251	-11.75	-12.956	-14.48	-15.936
-9.4392	-10.516	-11.226	-11.427	-11.171	-10.724	-10.473	-10.703	-11.46	-12.575	-13.802
-9.7812	-10.475	-10.847	-10.852	-10.564	-10.177	-9.933	-10.022	-10.504	-11.306	-12.285
-9.8433	-10.279	-10.452	-10.362	-10.081	-9.7471	-9.5226	-9.5374	-9.8464	-10.423	-11.187
-9.7565	-10.019	-10.076	-9.9421	-9.6806	-9.3918	-9.1883	-9.1621	-9.3602	-9.7776	-10.37
-9.5915	-9.7399	-9.7272	-9.5753	-9.3363	-9.0845	-8.9004	-8.8513	-8.976	-9.2793	-9.7373
-9.3871	-9.4591	-9.4052	-9.2483	-9.0308	-8.8088	-8.6416	-8.5793	-8.6539	-8.8743	-9.2287

Appendix D: Normal stress in Y-direction, N/m², at trailing edge, *f* = 0.2

-5.69E-02	-0.19496	-0.33796	-1.7401	1.4857	-41.638	-60.696	-49.234	-46.942	-44.525	-43.2
-0.25402	-0.46066	-0.86754	-2.2524	-5.5898	-38.281	-55.444	-49.469	-46.57	-44.474	-43.098
-0.88189	-1.4924	-2.8267	-5.6513	-15.553	-33.123	-45.943	-47.756	-45.717	-44.127	-42.862
-2.01	-3.2671	-5.5802	-10.505	-19.365	-30.33	-39.325	-43.599	-44.049	-43.257	-42.394
-3.5279	-5.3839	-8.534	-13.628	-20.699	-28.618	-35.408	-39.699	-41.533	-41.834	-41.534
-5.1832	-7.4651	-10.839	-15.506	-21.267	-27.362	-32.768	-36.709	-39.02	-40.065	-40.355
-6.7785	-9.2364	-12.534	-16.69	-21.475	-26.401	-30.864	-34.396	-36.824	-38.268	-39.003
-8.1987	-10.674	-13.776	-17.456	-21.517	-25.63	-29.419	-32.579	-34.964	-36.6	-37.624
-9.4179	-11.824	-14.696	-17.965	-21.475	-24.997	-28.281	-31.121	-33.4	-35.106	-36.305
-10.448	-12.743	-15.387	-18.31	-21.39	-24.464	-27.359	-29.928	-32.081	-33.789	-35.305
-11.312	-13.482	-15.914	-18.547	-21.285	-24.01	-26.595	-28.936	-30.959	-32.634	-33.97

Appendix E: Shear stress in XY-direction, N/m², at trailing edge, *f* = 0.2

-0.27057	-0.43604	-0.79683	-1.6612	-8.231	-11.755	-4.9812	-1.0052	-1.3442	-1.2672	-1.1168
-0.92088	-1.4443	-2.4629	-4.9859	-11.317	-13.699	-7.26	-2.1156	-1.1502	-0.91238	-0.75128
-2.5619	-3.813	-6.0191	-10.052	-14.696	-15.321	-10.488	-4.9109	-2.0269	-1.0015	-0.5596
-4.5652	-6.3654	-9.035	-12.342	-14.823	-14.686	-11.69	-7.531	-4.19	-2.2612	-1.2557
-6.42	-8.3627	-10.722	-13.029	-14.415	-14.086	-11.996	-8.9705	-6.0557	-3.8588	-2.4205
-7.8804	-9.6649	-11.547	-13.142	-13.94	-13.562	-12.023	-9.7534	-7.3509	-5.2661	-3.6709
-8.9271	-10.456	-11.916	-13.031	-13.499	-13.127	-11.939	-10.186	-8.2238	-6.367	-4.7959
-9.6435	-10.916	-12.044	-12.837	-13.112	-12.763	-11.816	-10.424	-8.8125	-7.1982	-5.7345
-10.12	-11.167	-12.044	-12.619	-12.775	-12.456	-11.681	-10.551	-9.213	-7.8195	-6.4924
-10.428	-11.289	-11.977	-12.4	-12.483	-12.193	-11.546	-10.611	-9.487	-8.2839	-7.096
-10.619	-11.33	-11.875	-12.191	-12.227	-11.964	-11.415	-10.629	-9.6743	-8.6317	-7.5738

Appendix F: Normal stress in X-direction, N/m², at trailing edge, *f* = 0.4

12.556	12.823	13.073	13.248	7.1678	-7.838	-18.156	-17.849	-15.449	-14.485	-14.016
8.1103	7.2118	5.5605	1.7944	-2.0909	-2.9902	-4.7892	-8.767	-11.052	-11.668	-12.035
4.3102	2.8496	-0.69852	-1.411	-2.4092	-2.7212	-3.2524	-4.8	-7.0608	-8.8005	-9.8677
1.4931	6.63E-02	-1.3903	-2.4472	-2.849	-2.7757	-2.9245	-3.7681	-5.1802	-6.7426	-8.0722
-0.42516	-1.5187	-2.4546	-3.0199	-3.1403	-3.0287	-3.0546	-3.5152	-4.44	-5.6193	-6.8223
-1.6916	-2.4902	-3.0921	-3.3998	-3.4353	-3.317	-3.3074	-3.5841	-4.199	-5.0717	-6.0621
-2.5536	-3.1303	-3.5255	-3.7017	-3.6913	-3.6037	-3.5868	-3.766	-4.1935	-4.8414	-5.634
-3.1624	-3.5826	-3.8504	-3.9564	-3.9365	-3.8697	-3.8559	-3.9813	-4.291	-4.7813	-5.4124
-3.609	-3.9204	-4.1084	-4.1762	-4.1568	-4.1082	-4.1002	-4.1945	-4.4279	-4.807	-5.3125
-3.9471	-4.1827	-4.3194	-4.3661	-4.3506	-4.3167	-3.3416	-4.3897	-4.5718	-4.8712	-5.2801
-4.2089	-9.0102	-4.4939	-4.5284	-4.5176	-4.4949	-4.4877	-4.56	-4.7061	-4.9471	-5.2813

Appendix G: Normal stress in Y-direction, N/m², at trailing edge, *f* = 0.4

-2.36E-02	-0.10159	-1.39E-03	-0.99606	9.33E-01	-24.853	-3.85E+01	-33.335	-3.32E+01	-32.709	-3.28E+01
-0.13085	-0.24875	-0.48395	-1.2979	-3.2751	-23.068	-35.187	-33.296	-32.79	-32.55	-32.608
-0.48788	-0.84905	-1.6463	-3.3512	-9.3694	-20.425	-29.361	-31.94	-31.974	-32.066	-32.213
-1.1616	-1.9254	-3.3428	-6.3779	-11.949	-19.126	-25.497	-29.252	-30.697	-31.261	-31.661
-2.1031	-3.2571	-5.2295	-8.4603	-13.048	-18.386	-23.295	-26.866	-29.002	-30.169	-30.891
-3.1647	-4.6133	-6.7764	-9.8151	-13.656	-17.878	-21.86	-25.088	-27.394	-28.932	-29.969
-4.222	-5.815	-7.9772	-10.749	-14.02	-17.514	-20.862	-23.75	-26.032	-27.735	-28.99
-5.1969	-6.8337	-8.9116	-11.421	-14.261	-17.243	-20.132	-22.726	-24.907	-26.658	-28.038
-6.0652	-7.6871	-9.65	-11.927	-14.433	-17.037	-19.581	-21.927	-23.983	-25.72	-27.156
-6.8277	-8.4036	-10.245	-12.322	-14.565	-16.878	-19.154	-21.291	-23.222	-24.911	-26.361
-7.4948	-9.0102	-10.736	-12.64	-14.671	-16.756	-18.816	-20.779	-22.59	-24.218	-25.655

Appendix H: Shear stress in XY-direction, N/m², at trailing edge, *f* = 0.4

-1.58E-02	-9.29E-02	-0.27656	-0.73692	-4.5579	-6.6844	-2.5217	0.24947	0.36981	0.65907	0.96248
-0.30448	-0.59165	-1.1695	-2.6445	-6.4442	-8.0426	-4.2367	-0.87693	3.92E-02	0.46817	0.81463
-1.1511	-1.8866	-3.209	-5.6747	-8.6426	-9.3344	-6.6494	-3.224	-1.2197	-0.29752	0.25595
-2.3318	-3.4381	-5.1062	-7.235	-8.9691	-9.1775	-7.5903	-5.1261	-2.9772	-1.5792	-0.70796
-3.5091	-4.7475	-6.2861	-7.8592	-9	-8.9986	-7.9405	-6.1979	-4.3888	-2.9096	-1.8299
-4.5018	-5.6821	-6.9661	-8.1253	-8.8381	-8.8415	-8.0979	-6.8274	-5.3754	-4.0251	-2.9057
-5.2722	-6.3226	-7.3685	-8.239	-8.7378	-8.722	-8.1758	-7.2227	-6.0651	-4.8958	-3.8373
-5.8541	-6.7641	-7.6157	-8.2868	-8.654	-8.6344	-8.2211	-7.4878	-6.5595	-5.5669	-4.61
-6.2927	-7.0748	-7.7747	-8.3063	-8.589	-8.5722	-8.2527	-7.6769	-6.9253	-6.0879	-5.2419
-6.6265	-7.2992	-7.8824	-8.3142	-8.5407	-8.5294	-8.2788	-7.8193	-7.2047	-6.498	-5.758
-6.8842	-7.4662	-7.959	-8.318	-8.506	-8.5011	-8.3027	-7.9313	-7.424	-6.8259	-6.1816

Appendix I: Normal stress in X-direction, N/m², at trailing edge, *f* = 0.8

24.296	25.306	26.461	27.813	29.448	31.554	35.44	40.623	41.774	37.793	32.565
22.466	23.271	24.171	25.292	26.376	27.851	28.87	28.902	28.896	28.17	25.59
20.485	21.048	21.638	22.24	22.822	23.126	22.998	22.653	22.143	21.279	20.055
18.431	18.75	19.033	19.242	19.285	19.083	18.647	18.07	17.464	16.779	15.863
16.386	16.486	16.513	16.424	16.178	15.758	15.2	14.586	13.972	13.351	12.643
14.414	14.34	14.179	13.908	13.513	13.004	12.24	11.817	11.235	10.669	10.075
12.561	12.36	12.076	11.701	11.237	10.701	10.128	9.5574	9.0135	8.4954	7.9727
10.85	10.563	10.025	8.333	9.2874	8.7556	8.2089	7.6744	7.169	6.6906	6.2182
9.2897	8.9479	8.5497	8.0997	7.0691	7.0956	6.5801	6.0819	5.6118	5.1675	4.7332
7.8781	7.5052	7.0887	6.6355	6.1569	5.6678	5.1844	4.7202	4.2821	3.8675	3.4643
6.6073	6.2195	5.7993	5.3541	4.8942	4.432	3.9797	3.5469	3.1378	2.7499	2.3734

Appendix J: Normal stress in Y-direction, N/m², at trailing edge, *f* = 0.8

2.92E-02	3.76E-02	4.65E-02	7.44E-02	7.00E-02	2.94E-01	-1.00E-01	4.33E+00	-7.07E-01	-6.27E+00	-9.83E+00
7.06E-02	8.83E-02	0.11375	0.15497	0.21988	0.3837	0.67252	3.3546	-0.20285	-5.2006	-8.9567
0.17885	0.21997	0.27847	0.36469	0.51153	0.74627	1.4711	1.8296	-3.00E-02	-3.7576	-7.5355
0.31796	0.38252	0.46898	0.59079	0.76049	1.0422	1.2786	0.87326	-0.70947	-3.4462	-6.7699
0.44962	0.52412	0.61617	0.7266	0.85564	0.94274	0.79271	-9.99E-02	-1.39E+00	-3.6868	-6.526
0.54307	0.6077	0.67419	0.73416	0.74434	0.62865	0.23649	-0.61424	-2.0516	-4.0777	-6.5584
0.5794	0.61423	0.63067	0.60473	0.4904	0.21005	-0.34306	-1.2788	-2.67E+00	-4.5108	-6.7224
0.55117	0.54161	0.49331	0.37713	0.147	-0.25964	-0.91915	-1.9008	-3.2455	-4.9478	-6.9525
0.45981	0.39764	0.28041	7.86E-02	-0.24831	-0.75023	-1.4804	-2.4838	-3.78E+00	-5.3751	-7.2163
0.31193	0.1946	1.07E-02	-0.26718	-0.67294	-1.2451	-2.0215	-3.0318	-4.2899	-5.7883	-7.4973
0.11641	-5.48E-02	-0.29984	-0.64272	-1.1113	-1.7349	-2.5408	-3.5487	-4.77E+00	-6.1868	-7.7865

Appendix K: Shear stress in XY-direction, N/m², at trailing edge, *f* = 0.8

-0.44229	0.49799	0.57019	0.6688	0.81365	1.0538	1.8968	2.0677	2.3322	4.4742	6.9123
0.82099	0.91738	1.04	1.2033	1.4342	1.8168	2.4547	2.3527	2.1431	3.3653	5.1942
1.4739	1.6257	1.8116	2.0445	2.3444	2.7215	2.8864	2.425	1.7455	1.747	2.5083
1.9152	2.072	2.2488	2.4424	2.6328	2.7154	2.4962	1.9204	1.2434	0.85961	0.97427
2.1508	2.2701	2.383	2.4686	2.5772	2.3228	1.93	1.3192	0.65313	0.16255	9.06E-03
2.2051	2.2607	2.2833	2.2443	2.0995	1.8004	1.324	0.71104	7.45E-02	-0.43791	-0.70585
2.113	2.095	2.0255	1.8789	1.6251	1.2413	0.72922	0.13115	-0.47034	-0.97363	-1.2907
1.9114	1.822	1.6721	1.4428	1.1166	0.68621	0.164	-0.41137	-0.97758	-1.4616	-1.7983
1.6331	1.481	1.2667	0.97765	0.60572	0.15233	-0.36617	-0.91611	-1.4494	-1.9118	-2.2543
1.3049	1.1011	0.83575	0.50736	0.10826	-0.35361	-0.86111	-1.3855	-1.8891	-2.3305	-2.6722
0.94717	0.70237	0.40281	4.54E-02	-0.36818	-0.82966	-1.3226	-1.8227	-2.2997	-2.7218	-3.0596

Appendix L: Normal stress in X-direction, N/m², at leading edge, *f* = 0.2

-62.113	-69.352	-79.537	-97.411	-115.49	-96.273	-45.287	-17.105	-12.967	-10.501	-8.788
-56.549	-60.799	-65.138	-64.74	-56.826	-53.767	-53.776	-42.198	-28.651	-21.723	-17.326
-48.716	-49.656	-48.349	-44.463	-41.856	-42.106	-42.891	-41.359	-35.512	-28.592	-23.493
-40.892	-39.83	-37.546	-35.092	-33.913	-34.773	-36.508	-36.777	-34.711	-30.904	-26.719
-34.293	-32.771	-30.893	-29.374	-29.037	-30.051	-31.644	-32.633	-32.165	-30.291	-27.612
-29.185	-27.783	-26.411	-25.56	-25.619	-26.594	-28.01	-29.132	-29.396	-28.639	-27.079
-25.28	-24.143	-23.206	-22.769	-23.025	-23.925	-25.153	-26.254	-26.828	-26.692	-25.888
-22.256	-21.39	-20.777	-20.6	-20.95	-21.769	-22.84	-23.862	-24.558	-24.76	-24.44
-19.863	-19.229	-18.85	-18.836	-19.229	-19.972	-20.914	-21.848	-22.575	-22.957	-22.94
-17.925	-17.476	-17.263	-17.353	-17.762	-18.439	-19.276	-20.125	-20.841	-21.314	-21.484
-16.317	-16.012	-15.919	-16.075	-16.485	-17.106	-17.856	-18.629	-19.316	-19.83	-20.114

Appendix M: Normal stress in Y-direction, N/m², at leading edge, *f* = 0.2

-63.46	-67.881	-74.835	-82.275	-109.65	-81.286	2.392	-3.6681	-0.18876	-0.46368	-0.16546
-63.505	-68.1	-74.555	-83.416	-100.46	-74.292	-11.659	-4.7978	-1.9388	-1.0642	-0.61366
-63.676	-68.237	-73.981	-81.581	-83.191	-63.055	-30.839	-11.586	-5.9479	-3.2394	-1.9731
-63.602	-67.561	-71.944	-74.678	-70.412	-56.41	-37.229	-20.776	-11.302	-6.773	-4.2699
-62.814	-65.761	-67.987	-67.624	-62.566	-52.222	-38.83	-26.191	-16.758	-10.784	-7.2086
-61.326	-63.099	-63.697	-62.022	-57.141	-49.07	-39.085	-29.117	-20.748	-14.547	-10.275
-59.371	-60.182	-59.795	-57.575	-53.127	-46.597	-38.754	-30.717	-23.478	-17.585	-13.107
-57.227	-57.35	-56.393	-54	-50.006	-44.57	-38.189	-31.552	-25.315	-19.914	-15.515
-55.075	-54.732	-53.462	-51.068	-49.489	-42.865	-37.532	-31.848	-26.538	-21.659	-17.483
-53.012	-52.362	-50.935	-48.618	-45.401	-41.398	-36.848	-32.057	-27.34	-22.953	-19.058
-51.079	-50.235	-48.741	-46.536	-43.629	-40.117	-36.169	-32.005	-27.851	-23.904	-20.303

Appendix N: Shear stress in XY-direction, N/m², at leading edge, *f* = 0.2

9.9139	9.8453	9.4925	7.8777	13.804	25.66	18.069	4.46	2.3971	1.5021	1.0604
7.9148	7.64	7.2727	7.878	16.391	28.436	23.955	11.357	6.1089	3.8904	2.7055
5.1063	5.0543	5.8772	10.158	20.221	30.053	29.842	21.325	13.467	9.0192	6.4234
4.3848	5.3638	8.0691	13.723	21.573	27.902	29.075	25.04	19.015	13.936	10.417
5.0091	6.9455	10.445	15.629	21.502	26.053	27.48	25.572	21.669	17.421	13.805
6.1813	8.5947	12.11	16.519	21.034	24.481	25.899	25.078	22.604	19.407	16.239
7.3963	9.9236	13.171	16.863	20.431	23.162	24.487	24.241	22.694	20.368	17.786
8.4511	10.903	13.806	16.907	19.803	22.036	23.252	23.321	22.372	20.705	18.668
9.2976	11.591	14.156	16.785	19.189	21.063	22.171	22.417	21.858	20.674	19.094
9.9468	12.053	14.317	16.57	18.604	20.207	21.219	21.563	21.265	20.432	19.217
10.428	12.347	14.439	16.302	18.051	19.447	20.372	20.769	20.647	20.07	19.143

Appendix O: Normal stress in X-direction, N/m², at leading edge, *f* = 0.4

-73.394	-83.827	-98.743	-125.32	-157.43	-141.58	-75.053	-34.071	-26.737	-22.385	-19.353
-68.722	-75.735	-83.57	-86.148	-78.41	-75.893	-77.526	-63.19	-45.042	-35.456	-29.255
-60.134	-62.775	-62.722	-59.126	-56.816	-58.049	-59.876	-58.669	-51.559	-42.624	-35.898
-50.825	-50.534	-48.588	-46.225	-45.3	-46.922	-49.749	-50.716	-48.577	-44.003	-38.744
-42.629	-41.428	-39.659	-38.2	-38.144	-39.81	-42.28	-44.042	-43.918	-41.889	-38.726
-36.115	-34.854	-33.532	-32.774	-33.121	-34.644	-36.786	-38.609	-39.355	-38.76	-37.068
-31.046	-29.982	-29.097	-28.781	-29.317	-30.687	-32.519	-34.238	-35.314	-35.477	-34.753
-27.07	-26.259	-25.711	-25.674	-26.291	-27.518	-29.101	-30.662	-31.837	-32.39	-32.265
-23.898	-23.259	-23.018	-23.154	-23.798	-24.9	-26.282	-27.687	-28.856	-29.601	-29.836
-21.315	-20.925	-20.804	-21.047	-21.691	-22.687	-23.907	-25.171	-26.29	-27.116	-27.563
-19.169	-18.931	-18.936	-19.245	-19.874	-20.78	-21.869	-23.009	-24.063	-24.911	-25.477

Appendix P: Normal stress in Y-direction, N/m², at leading edge, *f* = 0.4

-7.29E+01	-78.952	-8.85E+01	-99.109	-1.37E+02	-106.06	2.58E+00	-5.0311	-3.52E-01	-0.67102	-2.57E-01
-72.856	-79.213	-88.218	-100.88	-125.96	-96.847	-16.025	-6.6459	-2.7463	-1.5233	-0.8907
-73.122	-79.556	-87.899	-99.398	-104.54	-81.611	-40.964	-15.719	-8.1666	-4.5062	-2.7737
-73.326	-79.177	-86.002	-91.372	-88.196	-72.187	-48.591	-27.59	-15.205	-9.2086	-5.8625
-72.738	-77.419	-81.541	-82.702	-77.984	-66.247	-50.04	-34.228	-22.165	-14.406	-9.7137
-71.265	-74.484	-76.445	-75.691	-77.984	-61.767	-49.865	-37.596	-27.073	-19.156	-13.641
-69.146	-71.111	-71.706	-70.062	-65.559	-58.251	-49.022	-39.27	-30.301	-22.886	-17.186
-66.719	-67.755	-67.516	-65.498	-61.41	-55.37	-47.947	-39.996	-32.368	-25.66	-20.132
-64.22	-64.602	-63.871	-61.73	-58.047	-52.945	-46.805	-40.184	-33.654	-27.666	-22.479
-61.781	-61.714	-60.7	-58.562	-55.246	-50.859	-45.671	-40.057	-34.418	-29.092	-24.305
-59.467	-59.099	-57.93	-55.856	-52.861	-49.035	-44.574	-39.743	-34.828	-30.084	-25.703

Appendix Q: Shear stress in XY-direction, N/m², at leading edge, *f* = 0.4

1.73E+01	17.501	17.306	15.157	21.883	36.102	25.253	6.7099	3.6744	2.3471	1.6784
14.118	13.818	13.23	13.488	23.583	38.706	32.735	15.975	8.8091	5.7101	4.0312
9.2758	8.8809	9.3471	14.013	26.411	39.368	39.744	28.96	18.64	12.68	9.1525
7.1935	7.9575	10.805	17.503	27.413	35.871	37.952	33.204	25.593	19.007	14.374
7.0613	9.0616	13.065	19.382	26.885	33.02	35.329	33.326	28.596	23.254	18.617
7.8636	10.551	14.708	20.164	25.983	30.66	32.873	32.227	29.376	25.478	21.517
8.9026	11.818	15.732	20.351	24.983	28.704	30.733	30.777	29.114	26.377	23.229
9.8658	12.756	16.301	20.213	23.994	27.05	28.888	29.292	28.377	26.497	24.083
10.653	13.396	16.56	19.9	23.055	25.627	27.29	27.882	27.445	26.179	24.365
11.251	13.8	16.614	19.494	22.176	24.384	25.892	26.578	26.45	25.624	24.281
11.68	14.024	16.53	19.04	21.357	23.283	24.656	25.384	25.459	24.947	23.968

Appendix R: Normal stress in X-direction, N/m², at leading edge, *f* = 0.8

-95.497	-111.11	-133.92	-175.99	-235.06	-227.41	-131.88	-66.008	-52.585	-44.691	-39.201
-92.413	-104.15	-118.17	-126.2	-118.78	-117.36	-122.39	-103.02	-76.08	-61.433	-51.816
-82.475	-88.03	-90.124	-86.907	-85.052	-88.153	-92.018	-91.516	-82.064	-69.295	-59.473
-70.431	-71.395	-69.919	-67.592	-67.052	-70.066	-74.964	-77.279	-75.023	-68.998	-61.692
-59.254	-58.512	-56.82	-55.362	-55.752	-58.597	-62.701	-65.915	-66.442	-64.142	-60.021
-50.095	-48.988	-47.657	-46.986	-47.804	-50.308	-53.788	-56.916	-58.556	-58.253	-56.294
-42.818	-41.805	-40.934	-40.777	-41.782	-43.99	-46.927	-49.786	-51.785	-52.494	-51.901
-37.023	-36.245	-35.757	-35.926	-36.997	-38.95	-41.465	-44.015	-46.069	-47.263	-47.484
-32.349	-31.815	-31.616	-31.988	-33.064	-34.806	-36.987	-39.254	-41.223	-42.638	-43.327
-28.513	-28.193	-28.204	-28.699	-29.751	-31.317	-33.234	-35.254	-37.111	-38.581	-39.528
-25.313	-25.165	-25.426	-25.894	-26.908	-28.327	-30.031	-31.842	-33.564	-35.024	-36.101

Appendix S: Normal stress in Y-direction, N/m², at leading edge, *f* = 0.8

-91.818	-101.09	-115.56	-132.08	-190.49	-154.14	2.917	-7.681	-0.66045	-1.0683	-0.4284
-91.691	-101.35	-115.11	-134.85	-175.31	-140.56	-24.522	-10.222	-4.2978	-2.4005	-1.4169
-92.032	-101.95	-115.05	-133.81	-145.68	-117.45	-60.569	-23.694	-12.429	-6.9279	-4.2973
-92.658	-101.98	-113.3	-123.58	-122.43	-102.56	-70.481	-40.71	-22.696	-13.867	-8.8971
-92.371	-100.23	-107.83	-111.79	-107.65	-93.21	-71.586	-49.664	-32.532	-21.331	-14.491
-90.875	-96.729	-101.17	-102.08	-97.279	-86.166	-70.563	-53.858	-39.188	-27.97	-20.061
-88.408	-92.463	-94.827	-94.187	-89.503	-80.653	-68.732	-55.669	-43.365	-33.021	-24.972
-85.408	-88.094	-89.13	-87.739	-83.397	-76.144	-66.686	-56.188	-45.874	-36.648	-28.947
-82.242	-83.914	-84.12	-82.381	-78.431	-72.355	-64.629	-56.003	-47.291	-39.161	-32.025
-79.077	-80.037	-79.727	-77.854	-74.281	-69.101	-62.647	-55.424	-47.993	-40.848	-34.34
-76.029	-76.488	-75.862	-73.967	-70.738	-66.258	-60.77	-54.625	-48.223	-41.933	-36.042

Appendix T: Shear stress in XY-direction, N/m², at leading edge, *f* = 0.8

29.786	30.641	31.023	28.322	37.174	56.324	39.181	11.016	6.093	3.9357	2.8346
24.639	24.434	23.662	23.579	37.068	58.38	49.614	24.807	13.936	9.1455	6.523
16.38	15.469	15.405	20.931	37.896	56.974	58.603	43.519	28.471	19.61	14.302
12.012	12.458	16	24.403	38.302	50.897	54.786	48.72	38.091	28.622	21.86
10.647	12.825	17.834	26.34	36.981	46.175	50.205	48.046	41.753	34.324	27.736
10.893	14.138	19.542	27.01	35.329	42.364	46.108	45.809	42.246	37.014	31.537
11.708	15.386	20.584	26.974	33.636	39.248	42.621	43.219	41.336	37.811	33.582
12.582	16.322	21.095	26.553	32.019	36.637	39.656	40.693	39.838	37.543	34.403
13.322	16.932	21.239	25.93	30.51	34.403	37.111	38.353	38.136	36.705	34.435
13.874	17.272	21.135	25.203	29.112	32.459	34.899	36.225	36.408	35.581	33.981
14.245	17.402	20.867	24.43	27.818	30.742	32.955	34.299	34.734	34.33	33.239